CLASS GUIDELINE

DNVGL-CG-0038 Edition July 2019

Calculation of shafts in marine applications

The electronic pdf version of this document, available free of charge from http://www.dnvgl.com, is the officially binding version.

DNV GL AS

FOREWORD

DNV GL class guidelines contain methods, technical requirements, principles and acceptance criteria related to classed objects as referred to from the rules.

Any comments may be sent by e-mail to *rules@dnvgl.com*

CHANGES – CURRENT

This document supersedes the December 2015 edition of DNVGL-CG-0038.

Changes in this document are highlighted in red colour. However, if the changes involve a whole chapter, section or subsection, normally only the title will be in red colour.

Changes July 2019

Topic	*Reference*	*Description*
Alignment with IACS UR terms for tensile strength	Sec.1 [3]	Limits of application have been revised: — limit for material tensile strength is reduced from 1200 MPa to 950 MPa — limit for material yield strength (0.2% proof stress) is reduced from 900 MPa to 700 MPa. The fatigue calculations achieved by the procedures in this class guideline, are considered to be significantly more conservative than those achieved using the appendix in IACS UR M68. Hence, increased fatigue values may be utilized without performing fatigue testing.

Editorial corrections

In addition to the above stated changes, editorial corrections may have been made.

CONTENTS

SECTION 1 BASIC PRINCIPLES

1 Scope

This class guideline consists of the procedure and the basic equations for verification of the load carrying capacity for shafts. It is an S-N based methodology for fatigue life assessment mainly based on the DIN 743 Part 1 to 3: 2000-04 *Tragfähigkeits-berechnung von Wellen und Achsen* and VDEH 1983 Bericht Nr. ABF 11 *Berechnung von Wöhlerlinien für Bauteile aus Stahl, Stahlguss und Grauguss Synthetische Wöhlerlinien*.

However, it is "adapted and simplified" to fit typical shaft designs in marine applications, such as marine propulsion and auxiliaries on board ships and mobile offshore units.

Examples of introduced simplifications are that axial stresses are considered negligible for marine shafting systems as they are dominated by torsional- and bending stresses and direct use of mechanical strength from representative testing.

Even though such shafts are exposed to a wide spectrum of loads, just a few of the dominating load cases need to be considered instead of applying e.g. Miner's & Palmgrens's cumulative approach. These typical few load cases are described in [2] and illustrated in Figure 1.

The permissible stresses in the different shafts depend on the safety factors as required by the respective rule sections.

A recipe for how to assess the safety of surface hardened or peened shafts is given in this class guideline.

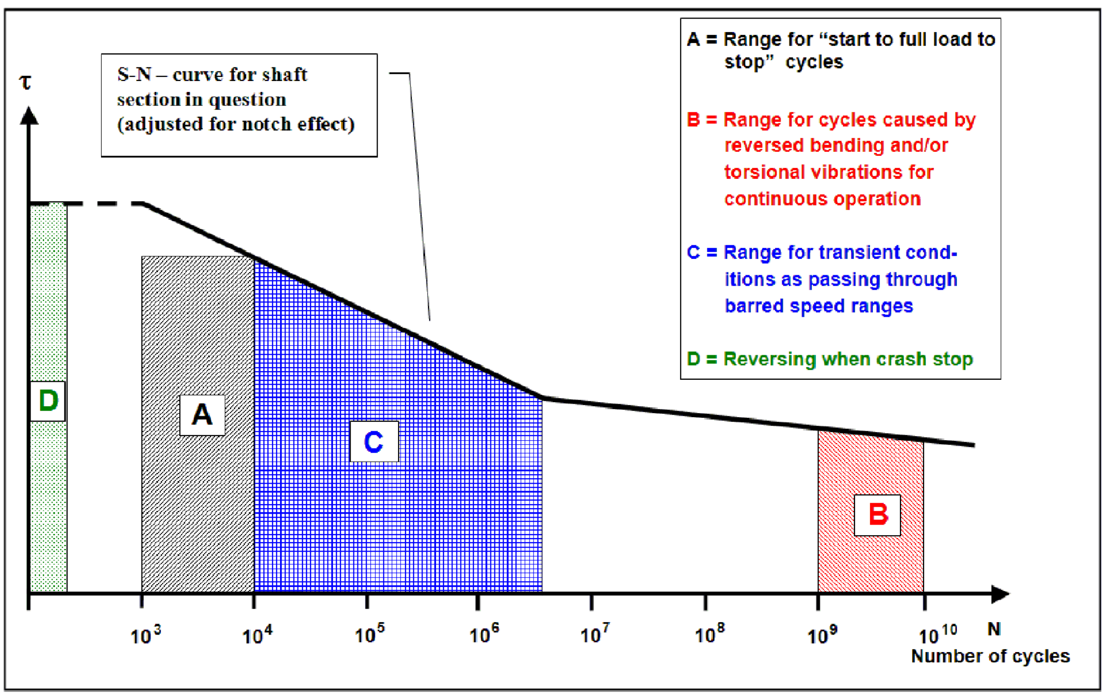

Figure 1 Applicable Load Cases (stress) and associated number of cycles

2 Description of method

Load case A

The criterion for this load case shall not be perceived as a design requirement versus static fracture or permanent distortion. Local yield will normally not be a decisive criterion for marine shafts. Much more relevant is the risk for Low Cycle Fatigue (LCF) failure. Cycling from stop (or idle speed) to a high operational speed, stresses the shaft material from zero stress to its maximum peak stress. A cycle is the completion of one repetition from zero (or idle speed) to a high operational speed and back to stop (or idle speed) again. This is often referred to as “primary cycles” comparable to the “Ground-Air-Ground cycles” (GAG) in the aircraft industry.

Peak loads that accumulate 10^3 to 10^4 load cycles during the life time of the ship should be considered for the LCF. For certain applications as e.g. short range ferries, higher number of cycles may have to be considered. For the “Low Cycle Fatigue criterion” presented in Sec.3 [2] a), 10^4 load cycles are used. Note that the considered maximum peak stress may not necessarily be associated with the maximum shaft speed, but could be an intermittent shock load, e.g. caused by a rapid clutching in or passing a main resonance, see Sec.3 Figure 1 to Sec.3 Figure 8.

Load case B

The criterion for this load case is introduced to prevent fatigue failure, caused by cyclic stresses, during normal and continuous operation (see also Sec.3 Figure 1 to Sec.3 Figure 8). The number of load cycles is associated with the total number of revolutions of the shaft throughout the vessels lifetime, which means up to or even more than 10^{10} load cycles, deserving its name; “High Cycle Fatigue (HCF) criterion”. The criterion is presented in Sec.4.

Load case C

This represents regular transient operations that are not covered by load case A, i.e. accumulates more than 10^4 load cycles during the life time of the ship. In practice for marine purposes, this means shafts in direct coupled propulsion plants driven by typically 5 to 8 cylinders diesel engine. The reason is that for such plants the engine’s main excitation order coincides with the first torsional natural frequency of the shafting system, where the “steady state” torsional vibration stress amplitudes normally exceeds the level determined by Load case B, see Sec.3 Figure 2, Sec.3 Figure 4 and Sec.3 Figure 8. A speed range around this resonance rpm shall be barred for continuous operation, and should only be passed through as quickly as possible, see Sec.3 Figure 5 to Sec.3 Figure 8. Still, certain plants may accumulate up to 1 million such load cycles during the life time of the ship. This is either caused by rather slow acceleration or deceleration, or frequent passing (e.g. manoeuvring speed below the barred speed range). On the other hand, optimized plants may accumulate as few cycles as 10^4 (e.g. plants with barred speed range in the lower region of the operational speed range or controllable pitch propeller (CPP) plants running through the barred speed range with zero or low pitch).

Load case D

This criterion serves the purpose of avoiding repeated yield reversals in highly loaded parts of the shaft. A yield reversal is defined as yield in tension followed by yield in compression or vice versa, Figure 2. All paper-clip bending mechanical engineers are well aware of that, after just a few cycles, their “workout” is terminated by an early failure of the clip. Such extreme loading regime is only applicable to shafts in plants with considerable negative torque, e.g. “crash stop” manoeuvres of reversible plants, see Sec.3 Figure 3 to Sec.3 Figure 8. These torque reversals are assumed to happen much less than 10^3 times.

For optimisation of a shafting system, in particular when transient operations are concerned, it is advised to use an iterative approach between dynamic analyses (as described in the *DNV GL rules for classification of ships* DNVGL-RU-SHIP Pt.4 Ch.2 Sec.2) and shaft design as presented in this class guideline.

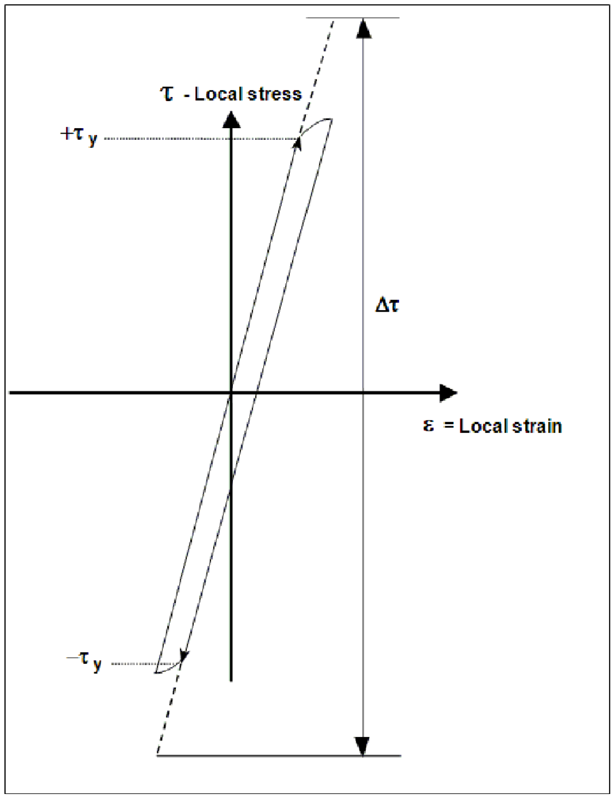

Figure 2 Hysteresis loops of plastification in the notch

Simplified diameter formulae are presented in the DNVGL-RU-SHIP Pt.4 Ch.4 Sec.1 [2.2.6] to DNVGL-RU-SHIP Pt.4 Ch.4 Sec.1 [2.2.8] for various common shaft designs. However, since the simplifications are made “to the safe side”, these formulae will result in somewhat larger dimensions than the basic criteria presented here.

For the purpose of demonstration, a few examples of the calculation methods are presented in App.A.

3 Limits of application

The criteria presented in this class guideline apply to shafts with:

— material of forged or hot rolled steels with minimum tensile strength of 400 MPa
— material tensile strength, σ_B up to 950 MPa and yield strength (0.2% proof stress), σ_y up to 700 MPa[1]
— no surface hardening[2]
— no chrome plating, metal spraying, welds etc. (which will require special considerations)
— protection against corrosion (through oil, oil based coating, paint, material selection or dry atmosphere)[3]

[1] For applications where it may be necessary to take the advantage of tensile strength above 800 MPa and yield strength above 600 MPa, material cleanliness has an increasing importance. Higher cleanliness than specified by material standards is required. See also DNVGL-RU-SHIP Pt.4 Ch.2 Sec.1 [5].

[2] However, some general guidelines are given in Sec.3 [6] and Sec.4 [5]

[3] For steels as those mentioned in footnote 1) special protection against corrosion is required. Method of protection shall be approved.

σ_y = yield strength or 0.2% proof stress limited to 0.7 σ_B. This limitation is introduced for the calculation purpose only, since further 'irrational' increase item of the yield stress (by the steel heat treatment) increase the risk of brittle fracture.

The fatigue calculations achieved by the procedures in this class guideline, are considered to be significantly more conservative than those achieved by using the appendix in IACS UR M68. Hence, the above may be used without performing fatigue testing.

Documenting the fatigue strength of the actual shaft, by performing representative torsional fatigue tests for low cycle and high cycle fatigue strength in notched and un-notched material (as required in IACS UR M68, details to be agreed with the Society), may be used two justify higher allowable stressed than those achieved using above procedure.

SECTION 2 NOMENCLATURE

1 Symbols

The symbols in Table 1 are used. Only SI units are used.

Table 1 Symbols

Symbol	*Term*	*Unit*
α_t	Geometrical stress concentration factor, torsion	-
α_b	Geometrical stress concentration factor, bending	-
λ	Rotational speed ratio = n/n_0	-
$\Delta\tau$	Repetitive nominal torsional stress range	MPa (= N/mm^2)
τ	Nominal mean torsional stress at any load (or r.p.m.)	MPa (= N/mm^2)
τ_0	Nominal torsional stress at maximum continuous power	MPa (= N/mm^2)
$\tau_{ice\ rev}$	Torsional stress due to ice shock while running astern	MPa (= N/mm^2)
τ_{max}	Repetitive nominal peak torsional stress	MPa (= N/mm^2)
τ_{vT}	Permissible torsional vibration stress amplitude for transient condition	MPa (= N/mm^2)
$\tau_{max\ reversed}$	Maximum reversed torsional stress	MPa (= N/mm^2)
τ_v	Nominal vibratory torsional stress amplitude,	MPa (= N/mm^2)
τ_f	High cycle fatigue strength	MPa (= N/mm^2)
τ_{vHC}	Permissible high cycle torsional vibration stress amplitude	MPa (= N/mm^2)
τ_{vLC}	Permissible low cycle torsional vibration stress amplitude	MPa (= N/mm^2)
σ_b	Nominal reversed bending stress amplitude (rotating bending stress amplitude)	MPa (= N/mm^2)
σ_B	Ultimate tensile strength [1)]	MPa (= N/mm^2)
σ_f	High cycle bending fatigue strength	MPa (= N/mm^2)
σ_y	Yield strength or 0.2% proof stress [1)]	MPa (= N/mm^2)
b	Width of square groove (circlip)	mm
d	Minimum shaft diameter at notch	mm
d_i	Inner diameter of shaft at notch	mm
d_h	Diameter of hole	mm
D	Bigger diameter in way of notch	mm
e	Slot width	mm
$f_L(\alpha_t,\sigma_y)$	Notch sensitivity term for low cycle fatigue	-
$f_L(R_y,\sigma_B)$	Surface condition influence term for low cycle fatigue	-

Symbol	Term	Unit
$f_{H\tau}(\alpha_t,m_t)$	Notch influence term for high cycle torsional fatigue	-
$f_{H\sigma}(\alpha_b,m_b)$	Notch influence term for high cycle bending fatigue	-
$f_H(r)$	Size (statistical) influence term for high cycle fatigue	-
$f_{H\tau}(R_y,\sigma_B)$	Surface condition influence term for high cycle torsional fatigue	-
$f_{H\sigma}(R_y,\sigma_B)$	Surface condition influence term for high cycle bending fatigue	-
k_{ec}	Eccentricity ratio	-
ΔK_A	Application factor, torque range	-
K_A	Application factor, repetitive cyclic torques	-
K_{AP}	Application factor, temporary occasional peak torques	-
K_{Aice}	Application factor, ice shock torques	-
$K_{H\sigma}$	Component influence factor for high cycle bending fatigue	-
$K_{H\tau}$	Component influence factor for high cycle torsional fatigue	-
K_L	Component influence factor for low cycle fatigue	-
ℓ	Total slot length	mm
m_b	Notch sensitivity coefficient for high cycle fatigue (bending)	-
m_t	Notch sensitivity coefficient for high cycle fatigue (torsion)	-
n	Actual shaft rotational speed, r.p.m.	minutes^{-1}
n_0	Shaft rotational speed at maximum continuous power, r.p.m.	minutes^{-1}
N_C	Accumulated number of load cycles	-
N_e	Accumulated number of load cycles during one passage up and down	-
P	Maximum continuous power	kW
r	Notch radius	mm
r_{ec}	Radius to eccentric axial bore	mm
R_a	Surface roughness, arithmetical mean deviation of the profile	µm
R_y	Surface roughness, maximum height of the profile (peak to valley)	µm
S	Safety factor	-
t	Thickness	mm
T_V	Vibratory torsional torque amplitude, ref. DNVGL-RU-SHIP Pt.4 Ch.2 Sec.2 [1.2]	kNm
T_0	Torque at maximum continuous power	kNm
W_t	Cross sectional modulus (first moment of area), torsion	mm^3
1) For representative test pieces according to the DNVGL-RU-SHIP Pt.2 Ch.2 Sec.6. If the mechanical properties are based on separately forged test pieces, the achieved properties must be reduced empirically in order to represent the properties of the real shaft.		

SECTION 3 THE LOW CYCLE FATIGUE CRITERION AND TORQUE REVERSAL CRITERION

1 Scope and general remarks

The low cycle fatigue criterion (LCF) and the torque reversal criterion (load case A and D in Sec.1 [2], respectively) are applicable for shafts subject to load conditions, which accumulate less than 10^4 load cycles. Typical such fatigue load conditions are:

Load variations from

— zero to full forward load
— zero to peak loads such as clutching-in shock loads, electric motor start-up with star-delta shift, ice shock loads (applicable for ships with ice class notations), etc.
— full forward load to reversed load (<10^3 load cycles).

Bending stress is normally disregarded since they are associated with the number of shaft revolutions (rotary bending) and thus with High Cycle Fatigue; Load case B. Only stochastic bending stresses of relatively high amplitudes but few cycles should be taken into account for the LCF (e.g. stochastic bending stresses in water jet shafts due to aeration or cavitation, see [3] and the DNVGL-RU-SHIP Pt.4 Ch.4 Sec.1 [6.3] item 2).

A component influence factor for LCF takes into account the difference in LCF strength of the actual shaft section and a polished plain test specimen push-pull loaded, see [5]. The required safety factor as given in the prevailing DNVGL-RU-SHIP Pt.4 Ch.4 Sec.1 [2.2.3], is selected based on the uncertainties associated with the LCF criterion itself, the load prediction, the non-cumulative approach and last but not least, the consequence of failure of a shaft disrupting an essential function on board such as propulsion or power generation.

2 Basic equations

The peak stresses are limited to:

For all shafts:

$$\text{a)} \qquad \tau_{max} \le \frac{\sigma_y}{2SK_L}$$

Additionally, for shafts in plants with considerable negative torque:

$$\text{b)} \qquad \alpha_t \Delta\tau \le \frac{2\,\sigma_y}{S\sqrt{3}}$$

τ_{max} = repetitive nominal peak torsional stress according to [3]
$\Delta\tau$ = repetitive nominal torsional stress range according to [4]
σ_y = yield strength or 0.2% proof stress limited to $0.7\sigma_B$. This limitation is introduced for the calculation purpose only, since further "irrational" increase of the yield strength (by the steel heat treatment) increases the risk for brittle fracture.
S = required safety factor according to the *DNV GL rules for classification of ships*
K_L = component influence factor for low cycle fatigue according to [5]

α_t = Geometrical stress concentration factor in torsion, Sec.6.

However, b) is only applicable when the principal stress is reversed in connection with reversed torsion. I.e. not applicable to e.g. keyways and splines.

α_t shall be set to unity for shrink fits since the stress concentration factors in Sec.6 Table 3 mainly consider the risk for fretting.

3 Repetitive nominal peak torsional stress, τ_{max}

For geared plants:

τ_{max} = τ_0 K_A or τ_0 K_{AP} or τ_0 K_{Aice} whichever is the highest, see Figure 1 and Figure 3.

For direct coupled plants:

τ_{max} ≈ maximum value of (τ + τ_v) in the entire speed range (for fwd running) or $\tau_0 \cdot K_{Aice}$ whichever is the highest, see Figure 2.

τ_0 = nominal torsional stress at maximum continuous power calculated as:
K_A = application factor, repetitive cyclic torques defined as:

$$\frac{T_0\, 10^6}{W_t} = \frac{16\, d\, T_0\, 10^6}{\pi(d^4 - d_i^4)}$$

$$\frac{T_0 + T_v}{T_0} = \frac{\tau_0 + \tau_v}{\tau_0}$$

See the Society's document DNVGL-CG-0036

K_{AP} = application factor, temporary occasional peak torques, see the Society's document DNVGL-CG-0036
K_{Aice} = application factor, ice shock torques, see DNVGL-RU-SHIP Pt.6 Ch.6 and the Society's document DNVGL-CG-0036
τ_v = nominal vibratory torsional stress amplitude for continuous operation, alternatively, the representative transient vibratory stress amplitude when passing a barred speed range.

The influence of any stochastic bending moments of high amplitudes (but few cycles) may be taken into account simply by multiply τ_0 with:

$$\sqrt{1 + \frac{1}{3}\left(\frac{\sigma_{b,max}}{\tau_0}\right)^2}$$

$\sigma_{b,max}$ = nominal reversed bending stress amplitude due to maximum stochastic bending moments (maximum rotating bending stress amplitude)

This simplification is justified because the estimation of these stochastic bending moments is very uncertain and conservative, see DNVGL-RU-SHIP Pt.4 Ch.4 Sec.1 [6.3] item 2.

4 Repetitive nominal torsional stress range,

Only applicable to plants with considerable negative torque.

For reversible geared plants:

$$\Delta\tau = \tau_0 \Delta K_A$$

ΔK_A = Application factor, torque range defined as:

$$\Delta K_A = \frac{K_{A(P)(ice)}\tau_0 + \left|\tau_{max\ reversed}\right|}{\tau_0}$$

see Figure 3.

As a safe simplification it may be assumed that

$$\Delta K_A = 2K_A \text{ or } 2K_{AP}, \text{ or } K_{Aice} + K_{(AP)}$$

whichever is the highest.

For direct coupled plants:

$$\Delta\tau = \tau_{max} + |\tau_{max\ reversed}|$$

see Figure 4 to Figure 8.

τ_{max}	≈	maximum value of $(\tau + \tau_v)$ in the entire speed range (for forward running) or $\tau_0 K_{Aice}$ whichever is the highest
$\tau_{max\ reversed}$	=	maximum reversed torsional stress which is the maximum value of $(\tau + \tau_v)$ in the entire speed range (for astern running)
$\Delta\tau$	=	repetitive nominal torsional stress range is equal to the maximum forward torsional stress plus the absolute value of the maximum reversed torsional stress.

As a safe simplification it may be assumed that $\Delta\tau \approx (\tau + \tau_v)$ or,

$(\tau_0 K_{Aice} + (\tau + \tau_v)_{astern})$ whichever is the highest.

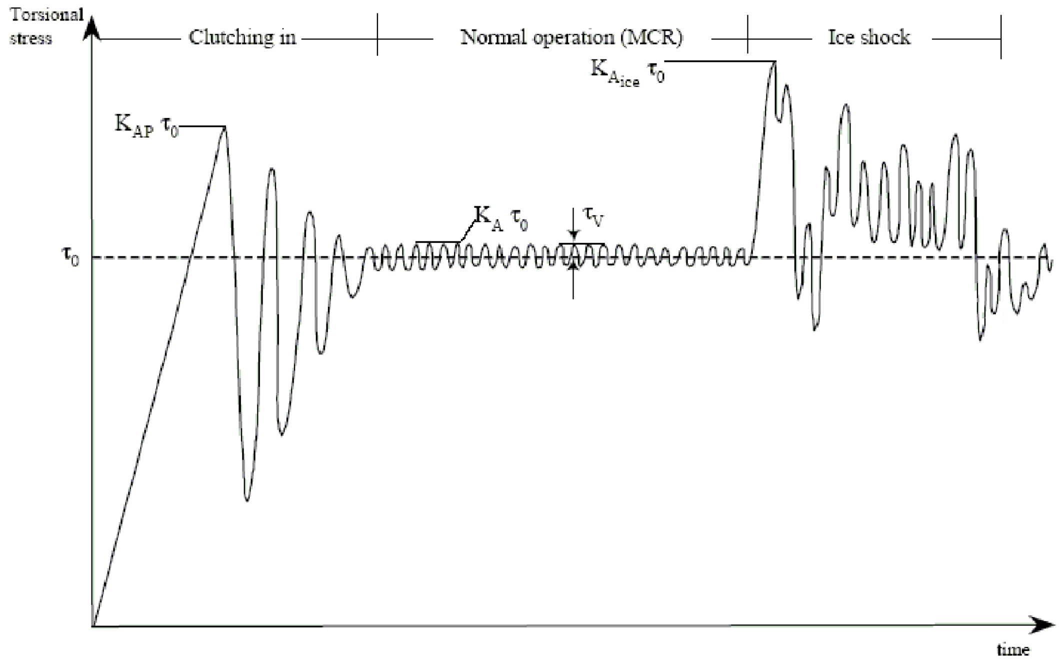

Figure 1 Typical torsional stresses in shafts for geared plants with unidirectional torque

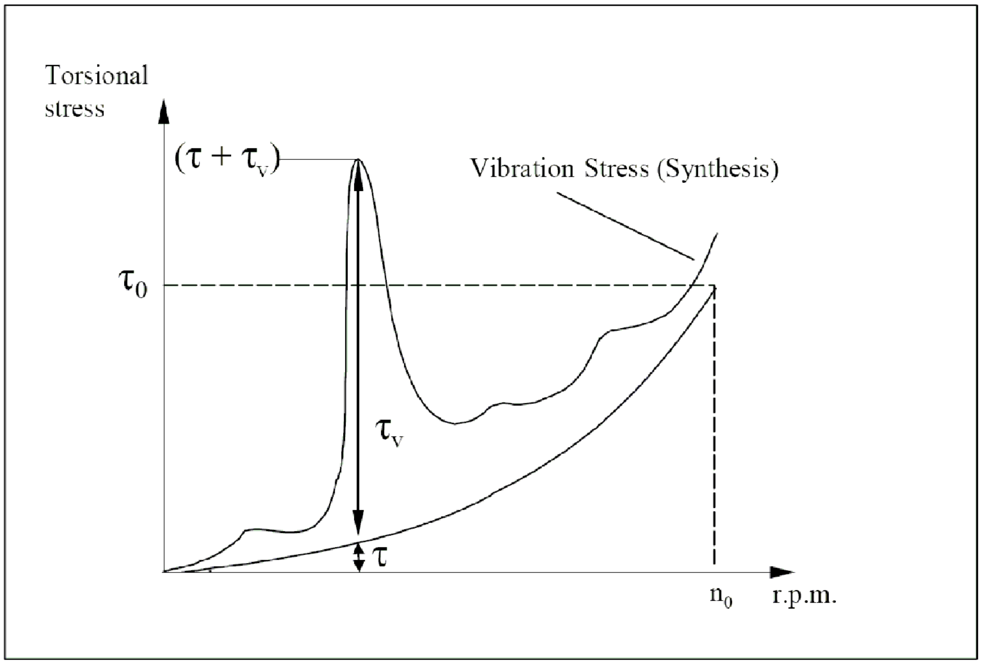

Figure 2 Typical torsional stresses in shafts for direct coupled plants, mean (τ) and upper stresses shown

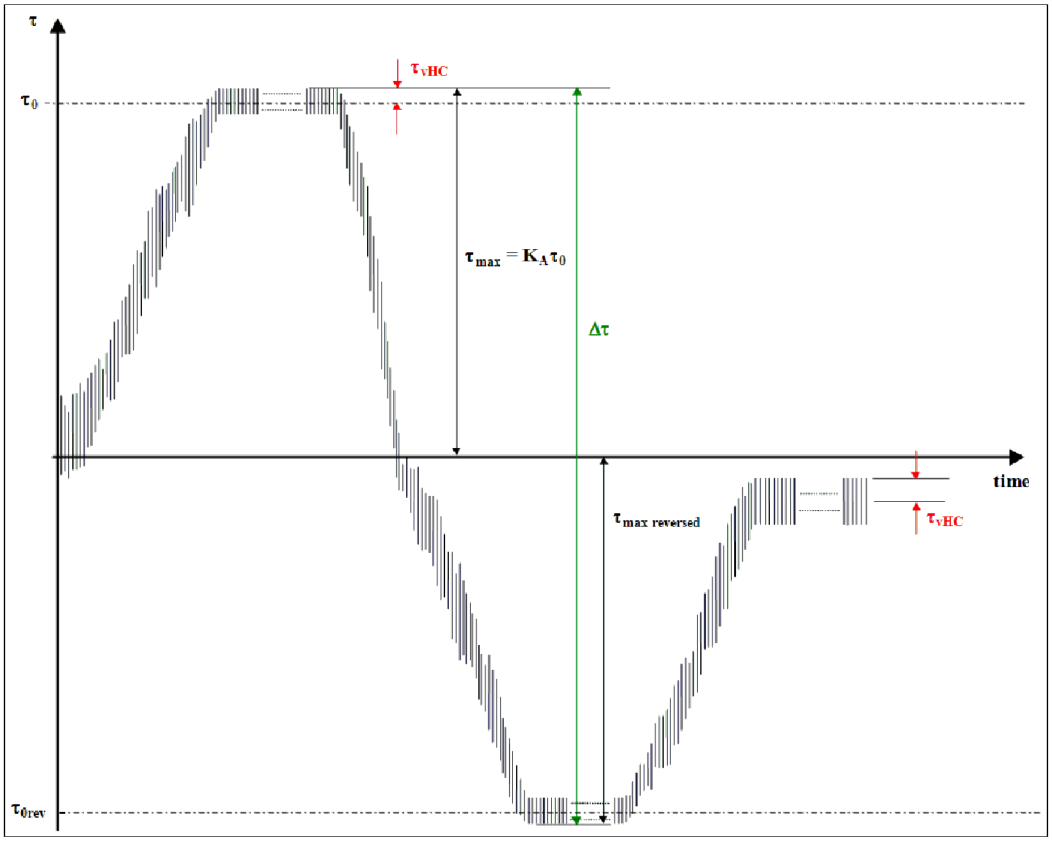

Figure 3 Stress range for reversible geared plants

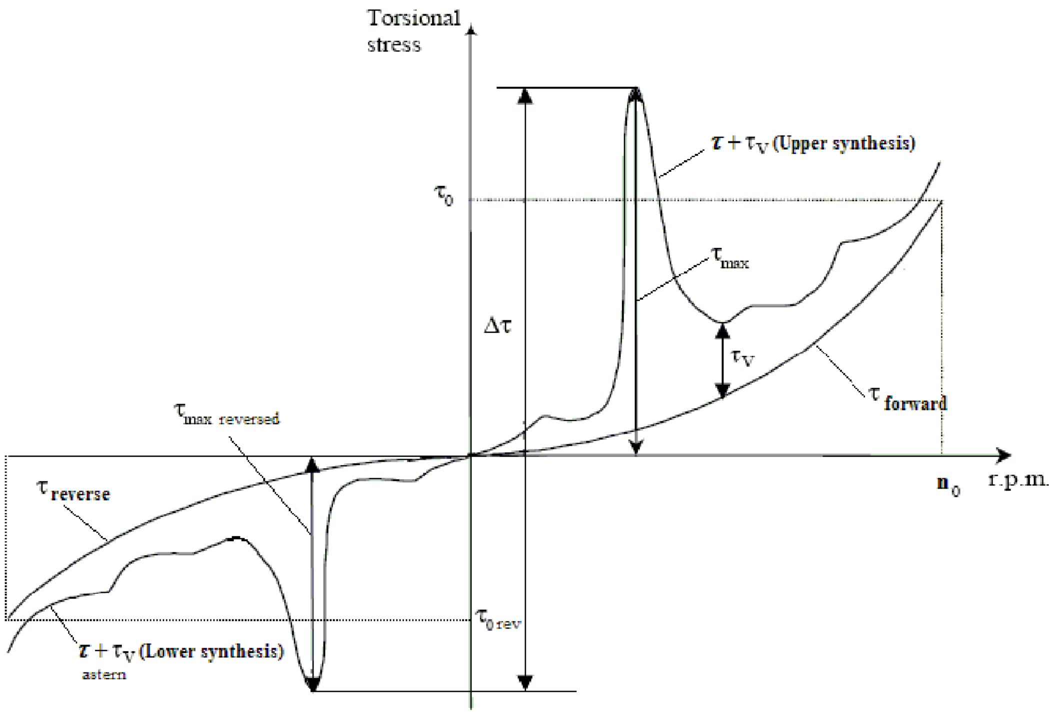

Figure 4 Stress range for direct coupled plants with respect to shaft speed, r.p.m.

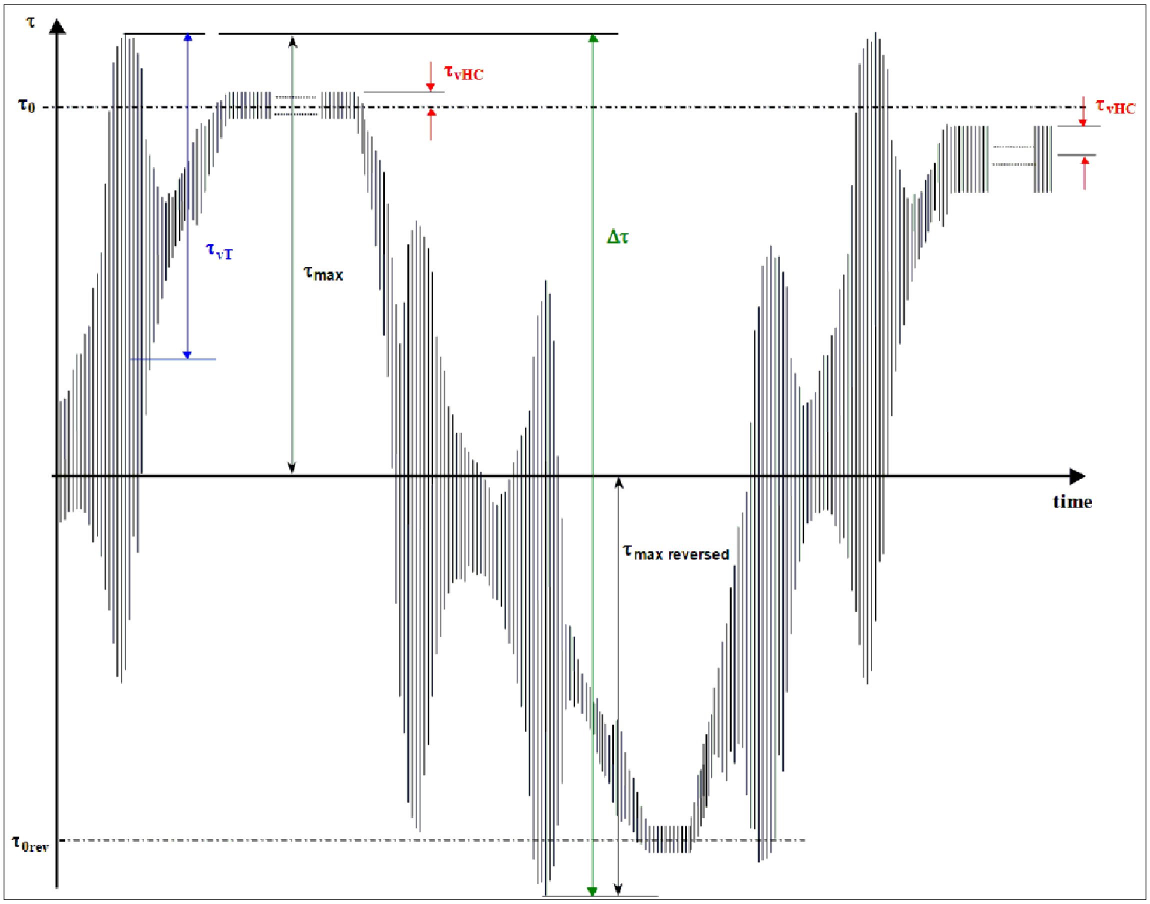

Figure 5 Stress range for direct coupled fixed pitch plants with respect to time (with high transient torsional stress amplitudes)

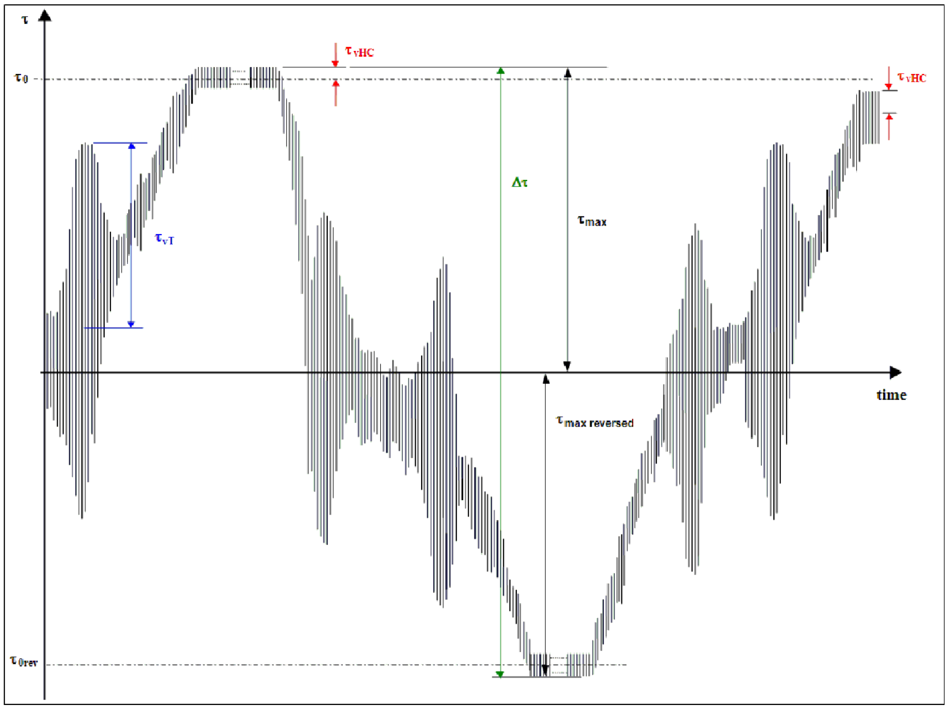

Figure 6 Stress range for direct coupled fixed pitch plants with respect to time (with low transient torsional stress amplitudes)

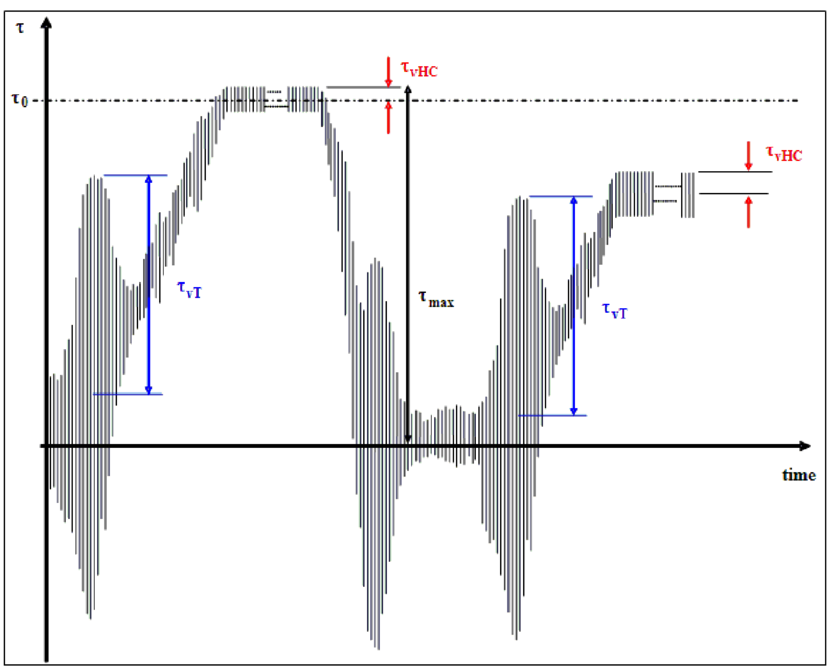

Figure 7 Stress range for direct coupled CP-propeller plants with respect to time

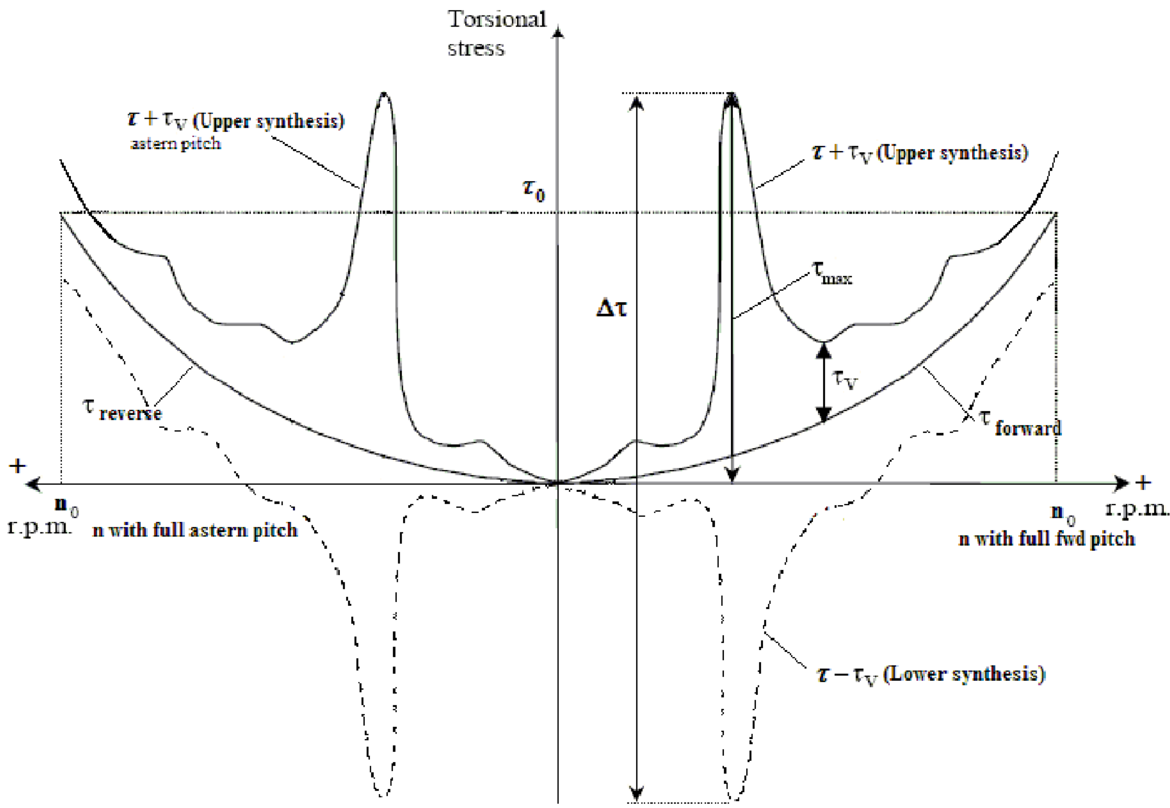

Figure 8 Stress range for direct coupled CP-propeller plants with respect to shaft speed, r.p.m.

5 Component Influence Factor for Low Cycle Fatigue, K_L

The component influence factor for low cycle fatigue takes into account the difference in fatigue strength of the actual shaft component and a polished plain test specimen push – pull loaded. The empirical formula is:

$$K_L = 1 + f_L(\alpha_t, \sigma_y) + f_L(R_y, \sigma_B)$$

$f_L(\alpha_t, \sigma_y)$	=	notch influence term for low cycle fatigue including notch sensitivity, see [5.1]
$f_L(R_y, \sigma_B)$	=	surface condition influence term for low cycle fatigue, see [5.2].

5.1 Notch influence term for low cycle fatigue, $f_L(\alpha_t, \sigma_y)$

This notch influence term is a simplified approach that reflects the increasing influence of a notch with increasing material strength:

$$f_L(\alpha_t,\sigma_y) = (\alpha_t - 1)\frac{\sigma_y}{900}$$

α_t = geometrical stress concentration factor, torsion according to 6

σ_y = yield strength or 0.2% proof stress (not limited to 0.7 σ_B).

5.2 Surface condition influence term for low cycle fatigue, $f_L(R_y,\sigma_B)$

This surface condition influence term is a simplified approach that reflects the increasing influence of surface roughness for high material strength.

For ordinary steels:

$$f_L(R_y,\sigma_B) = 10^{-4}(\sigma_B - 200)\log R_y$$

For stainless steel exposed to sea water:

$$f_L(R_y,\sigma_B) = 0.14 \log R_y$$

R_y = surface roughness, maximum height of the profile (i.e. peak to valley) ≈ $6R_a$. Minimum value to be used in the above formulae is R_Y = 1.0 μm

6 Surface Hardening/Peening

6.1 General remarks

Surface hardening is mainly applied in order to increase the strength in areas with stress concentrations. The increase is caused by higher hardness as well as compressive residual stresses.

Peening (e.g. cold rolling, shot peening, laser peening) is applied in order to induce compressive residual stresses (the work hardening effect is negligible). Both surface hardening and peening have a transition to the shaft core area where the compressive residual stresses shift into tensile stresses in order to balance the outer compressive stresses.

It is of vital importance that the applied working stresses do not alter the residual stresses in an unfavourable way, i.e. increasing residual tensile stresses. This is normally achieved by means of a minimum depth of hardening or peening. The basic principle is to calculate working stresses as a function of depth and to compare them with the assessed local strengths (hardness) and residual stresses along the same depth, see Figure 9.

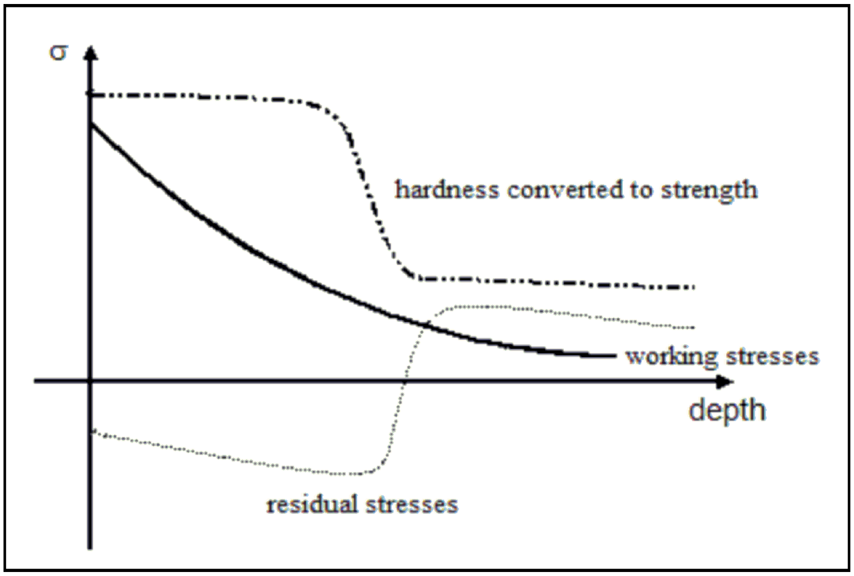

Figure 9 Local working- and residual stresses versus local strength (induction hardening shown)

A hardness profile (HV versus depth) can be converted to tensile strength (σ_B) as:

$$\sigma_B = 3.2HV$$

It is also of vital importance that the extension of hardening/peening in an area with stress concentration is duly considered. Any transition where the hardening/peening is ended is likely to have considerable tensile residual stresses. This forms a kind of "soft spot".

6.2 Calculation procedure

As of this time subject to special consideration.

SECTION 4 THE HIGH CYCLE FATIGUE CRITERION

1 Scope and general remarks

The high cycle fatigue criterion (HCF) is applicable for shafts subject to load conditions, which accumulate more than $3 \cdot 10^6$ load cycles, but typically 10^9 to 10^{10}. It is based on the combined vibratory torsional and rotating bending stresses (axial stresses disregarded) relative to the respective component fatigue strengths. Typical HCF load conditions are:

— Load variations due to torsional vibrations applicable for continuous operation (basically caused by engine firing pulses), and rotating bending moments due to forces from gear mesh and forces as listed in the DNVGL-RU-SHIP Pt.4 Ch.4 Sec.1 [6.3.1]).
— Load variations (torque and bending moment) due to ice impacts on the propeller for ice classed vessels assumed to accumulate $\sim 10^6$ load cycles, see the DNVGL-RU-SHIP Pt.6 Ch.6.

The fatigue strength is assumed to continuously drop beyond $3 \cdot 10^6$, i.e. no fatigue limit or run-out is assumed for the true shaft of ordinary grade for merchant steels. Since the HCF is associated with higher number of cycles than ordinary fatigue tests, which are terminated for practical considerations at about 10^8 cycles, it calls for a higher safety factor than for LCF. The prevailing safety factor for HCF is, in addition to the reasons mentioned in Sec.3 [1] for LCF, chosen due to:

— The statistical nature of fatigue, realizing that the S-N curve is drawn as an average, best fit curve determined with only a few test specimens. Even for plain test specimen the fatigue data contain considerable scatter and the standard deviation increases with number of cycles
— The inclusions in steel that have an important effect on the fatigue strength and its variability, but even vacuum re-melted steel shows significant scatter in fatigue strength
— The shortcomings of the commonly used NDT-methods in the marine industry (ultrasonic- and surface crack testing) and its workmanship on sized shafts (i.e. probability to detect defects)
— Corrosion. Even though the shaft surface has some corrosion protection (e.g. Dinol or Tectyl), there is always, after long time operation, a risk of corrosion on the surface of inboard shafts, which considerably reduces the high cycle fatigue strength.

Simplified diameter formulae are given in the DNVGL-RU-SHIP Pt.4 Ch.4 Sec.1 [4.4.1] to DNVGL-RU-SHIP Pt.4 Ch.4 Sec.1 [2.2.5] for various common shaft designs. However, since the simplifications are made “to the safe side”, these formulae will result in somewhat larger dimensions than the basic criteria presented here.

2 Basic Equation

The high cycle dynamic stresses are limited to:

$$\left(\frac{\tau_v}{\tau_f}\right)^2 + \left(\frac{\sigma_b}{\sigma_f}\right)^2 \le \frac{1}{S^2}$$

τ_v = nominal vibratory torsional stress for continuous operation.

For geared plants: τ_0 (K_A- 1) unless a higher value applies below the full speed range (~90% to 100% engine speed). K_A shall not be taken lower than 1.1 in order to cover for load fluctuations due to navigational commands and “rough sea hunting”.

For ice class: As long as the natural frequency of the “propeller versus engine”-mode is much lower than the propeller blade passing frequency

(ratio < 50%): 0.5 τ_0 (K_{Aice} − 1), otherwise:

τ_0 (K_{Aice} - 1)

τ_f = high cycle torsional fatigue strength, see [3]

σ_b = nominal reversed bending stress amplitude, see [1]

σ_f = high cycle bending fatigue strength, see [3]

S = required safety factor according to the *DNV GL rules for classification of ships* .

3 High Cycle Fatigue Strengths, τ_f and σ_f

The correlation between fatigue strength and mechanical strength is a simple function of the yield strength (or 0.2% proof stress). For ordinary steels, the high cycle fatigue strengths in bending and torsion are based on empirical formulae. For reversed stresses, the fatigue strength is presented as a linear function (e.g. 0.4 σ_y+70) of the main parameter which is assumed to be the yield strength (see VDEH 1983). These "weighted line of best fit" equations are based on a systematic collection of push-pull fatigue strength test results, each with 50% survival probability, of different types of steel, see VDEH 1983. Since these empirical formulas represent an "average" of average fatigue values, they have been reduced by 10%.

The mean stress influence is in principle the applied equivalent (von Mises) mean stress, but for marine shafting this means in practice a function of the mean torsional stress. Finally, the fatigue strengths are reduced by the component influence factor.

For stainless steel operating in seawater, the fatigue strengths are dependent on the expected number of load cycles. Test results are used as basis for the given figures, but are somewhat on the safe side in order to compensate for the influence of the mean stress (thus the mean stress influence is not incorporated as a separate parameter in these formulae).

For stainless steel *not* exposed to corrosive environment (e.g. applicable to shaft section inside keyless couplings or keyway couplings with additional sealing), the criteria for ordinary steel apply.

Table 1 Fatigue strengths

Material	*Cycles*[1)]	
	≈10^8	*10^9 to 10^{10}*
Ordinary steels	$\tau_f = \frac{0.24\,\sigma_y + 42 - 0.15\,\tau}{K_{H\tau}}$	
	$\sigma_f = \frac{0.4\,\sigma_y + 70 - 0.4\,\tau}{K_{H\sigma}}$	

Material	*Cycles*[1)]	
	≈10^8	*10^9 to 10^{10}*
Stainless steel I[2)] (in sea water)	$\tau_f = \frac{105}{K_{H\tau}}$	$\tau_f = \frac{90}{K_{H\tau}}$
	$\sigma_f = \frac{165}{K_{H\sigma}}$	$\sigma_f = \frac{140}{K_{H\sigma}}$
Stainless steel II[2)] and III[2)] (in sea water)	$\tau_f = \frac{118}{K_{H\tau}}$	$\tau_f = \frac{97}{K_{H\tau}}$
	$\sigma_f = \frac{184}{K_{H\sigma}}$	$\sigma_f = \frac{150}{K_{H\sigma}}$

1) The number of cycles refers to those accumulated in the full load range. 10^8 is a suitable estimate for e.g. pleasure craft. 10^9 to 10^{10} should be used for ferries, etc.

2) Stainless steel I = austenitic steels with 16 to 18% Cr, 10 to 14% Ni and > 2% Mo with σ_B = 490 to 600 MPa and $\sigma_y > 0.45\ \sigma_B$

Stainless steel II = martensitic steels with 15 to 17% Cr, 4 to 6% Ni and > 1% Mo with σ_B = 850 to 1000 MPa and $\sigma_y > 0.75\ \sigma_B$

Stainless steel III – ferritic-austenitic (duplex) steels with 25 to 27% Cr, 4 to 7% Ni and 1 to 2% Mo with σ_B = 600 to 750 MPa and $\sigma_y > 0.65\ \sigma_B$.

For other kinds of stainless steel, special consideration applies to fatigue values and pitting resistance, see DNVGL-RU-SHIP Pt.4 Ch.4 Sec.1 [2.2.4]

σ_y = yield strength or 0.2% proof stress limited to 0.7 σ_B. This limitation is introduced for the calculation purpose only, since further "irrational" increase of the yield stress (by the steel heat treatment) increases the risk for brittle fracture.

$K_{H\tau}$ = component influence factor for high cycle torsional fatigue, see [4]

$K_{H\sigma}$ = component influence factors for high cycle bending fatigue, see [4]

τ = nominal mean torsional stress at any load (or r.p.m.).

4 Component influence factor for high cycle fatigue, $K_{H\tau}$ and $K_{H\sigma}$

The component influence factor for high cycle fatigue takes into account the difference in fatigue strength of the actual shaft component and a polished plain test specimen push – pull loaded. The empirical formulae are:

Torsion: $K_{H\tau} = f_{H\tau}(\alpha_t, m_t) + f_H(r) + f_{H\tau}(R_y, \sigma_B)$

Bending: $K_{H\sigma} = f_{H\sigma}(\alpha_b, m_b) + f_H(r) + f_{H\sigma}(R_y, \sigma_B)$

$f_{H\tau}(\alpha_t, m_t)$ = notch influence term for high cycle torsional fatigue, see [4.1]
$f_{H\sigma}(\alpha_b, m_b)$ = notch influence term for high cycle bending fatigue, see [4.1]
$f_H(r)$ = size (statistical) influence term for high cycle fatigue, see [4.2]
$f_{H\tau}(R_y, \sigma_B)$ = surface condition influence term for high cycle torsional fatigue, see [4.3]
$f_{H\sigma}(R_y, \sigma_B)$ = surface condition influence term for high cycle bending fatigue, see [4.3].

4.1 Notch influence term for high cycle fatigue, $f_{H\tau}(\alpha_t, m_t)$ and $f_{H\sigma}(\alpha_b, m_b)$

This term represents the influence of the geometrical stress concentration, α and the notch sensitivity, m, which represents the notch factor when they are combined as

$$\frac{\alpha}{m}$$

For multi-radii transitions, see Sec.6 Table 1, resulting in low geometrical stress concentration factors ($\alpha_t \sim 1.05$ and $\alpha_b \sim 1.10$),

m_t and m_b are, as for a plain shaft, = 1.0.

If the calculated value of $f_{H\tau}(\alpha_t, m_t)$ or $f_{H\sigma}(\alpha_b, m_b)$ is below unity, the value 1.0 shall be used.

Torsion:

$$f_{H\tau}(\alpha_t, m_t) = \frac{\alpha_t}{m_t}$$

α_t = geometrical stress concentration factor, torsion according to 6
m_t = notch sensitivity coefficient for high cycle torsional fatigue, calculated as:

$$m_t = 1 + \left(\frac{60}{\sigma_y} - 0.05\right)\sqrt{\frac{1}{r}}$$

σ_y = yield strength or 0.2% proof stress (not limited to 0.7 σ_B).

Bending:

$$f_{H\sigma}(\alpha_b, m_b) = \frac{\alpha_b}{m_b}$$

α_b = geometrical stress concentration factor, bending according to Sec.6

m_b = notch sensitivity coefficient for high cycle bending fatigue, calculated as:

$$m_b = 1 + \left(\frac{60}{\sigma_y} - 0.05\right)\sqrt{\frac{2}{r}}$$

σ_y = yield strength or 0.2% proof stress (not limited to 0.7 σ_B).

4.2 Size (statistical) influence term for high cycle fatigue, $f_H(r)$

This term represents a size factor, which qualitatively takes into account the amount of material subject to high stresses. It does *not* represent the stress gradient influence since that is included in the notch sensitivity coefficient, m, above. Further, it does *not* consider the reduced material strength due to size since that is covered by requirements for testing representative specimen from forgings.

$$f_H(r) = 0.01\sqrt{r}$$

r = notch radius (use $d_h/2$ or e/2 for radial holes or slots, respectively, see Sec.6 [7] or Sec.6 [8]) or shaft radius whichever is smaller. If r >100, 100 shall be used.

4.3 Surface condition influence term for high cycle fatigue, $f_{H\tau}(R_y,\sigma_B)$ and $f_{H\sigma}(R_y,\sigma_B)$

This term takes the surface roughness into account. The surface roughness due to the machining constitutes a kind of stress concentration and reduced fatigue strength compared with a polished test specimen. The surface condition influence is higher for more notch sensitive, high strength steels.

For ordinary steels:

Torsion: $f_{H\tau}(\mathrm{R_y},\sigma_B) = 3\cdot 10^{-4}\,(\sigma_B - 200)\log \mathrm{R_y}$

Bending: $f_{H\sigma}(\mathrm{R_y},\sigma_B) = 4\cdot 10^{-4}\,(\sigma_B - 200)\log \mathrm{R_y}$

For stainless steel exposed to sea water:

Torsion and Bending: $f_{H\tau}(\mathrm{R_y},\sigma_B) = f_{H\sigma}(\mathrm{R_y},\sigma_B) = 0.35\log \mathrm{R_y}$

R_y = Surface roughness, maximum height of the profile (i.e. peak to valley) ≈ 6 R_a. Minimum value to be used in the above formulae is R_Y = 1.0 μm

5 Surface hardening/peening

5.1 General remarks

Surface hardening is mainly applied in order to increase the fatigue strength in areas with stress concentrations. The increase is caused by higher hardness as well as compressive residual stresses. Peening (e.g. cold rolling, shot peening, laser peening) is applied in order to induce compressive residual stresses (the work hardening effect is negligible). Both surface hardening and peening have a transition to the shaft core area where the compressive residual stresses shift into tensile stresses in order to balance the outer compressive stresses.

It is of vital importance that the extension of hardening/peening in an area with stress concentration is duly considered. Any transition where the hardening/peening is ended is likely to have considerable tensile residual stresses. This forms a kind of “soft spot”.

It is of vital importance that the applied dynamic working stresses do not exceed the local fatigue strengths, neither at the surface nor in the depth, especially at the transition to the core. This is may be achieved by means of a minimum depth of hardening or peening. The basic principle is to calculate both the mean and dynamic working stresses as functions of depth, see Figure 1. The residual stresses as a function of depth are then added to the mean working stresses. The local fatigue strength (for reversed stresses, i.e. R = – 1) is determined as a function of depth, depending on the local hardness and yield strength, respectively.

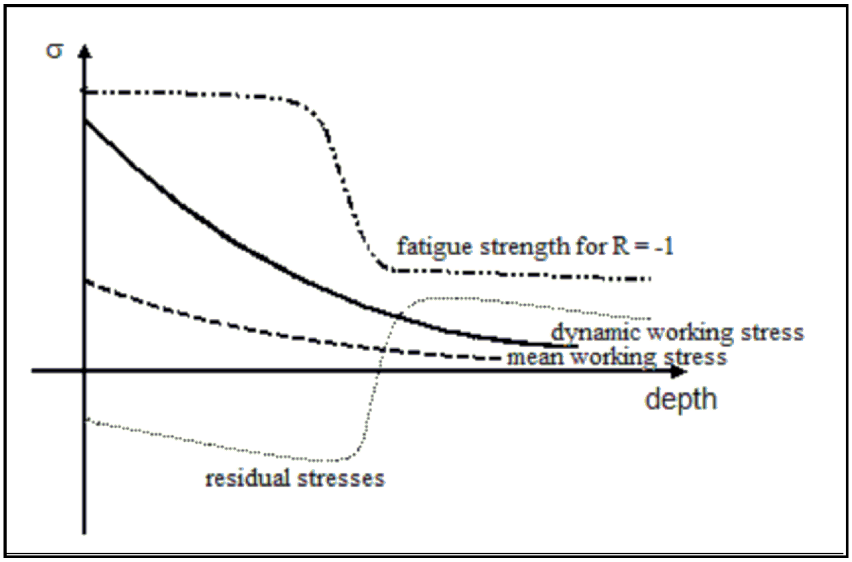

Figure 1 Local dynamic working stresses and residual stresses versus local fatigue strength (induction hardening shown)

The criterion for safety against fatigue is then applied stepwise from surface to core.

5.2 Calculation procedure

As of this time subject to special consideration.

SECTION 5 THE TRANSIENT VIBRATION CRITERION

1 Scope and general remarks

As mentioned in Sec.1 [2] load case C, the transient vibration criterion, which is applicable to vibration levels when passing through a barred speed range, applies in practice only to direct coupled plants.

The permissible torsional vibration stress amplitudes, τ_{vT} are determined by logarithmic interpolation between the low cycle criterion, LCF (τ_{vLC}) and the high cycle criterion, HCF (τ_{vHC}) (adjusted down to $3 \cdot 10^6$ load cycles simply by reducing the HCF safety factor to 1.5) depending on the foreseen accumulated number of cycles, N_C during the lifetime of the plant.

Barred speed ranges are only permitted below a speed ratio

$\lambda = n/n_0 = 0.8$ where n = actual r.p.m. and n_0 = r.p.m. at full power.

Simplified calculation method is given in the DNVGL-RU-SHIP Pt.4 Ch.4 Sec.1 [2.2.8] for some specific propeller and intermediate shaft designs under the assumption that the barred speed range is passed rapidly both upwards and downwards.

2 Basic equation

$$\tau_{vT} \leq \tau_{vHC}\left(\frac{3 \cdot 10^6}{N_C}\right)^{0.4\log\left(\frac{\tau_{vLC}}{\tau_{vHC}}\right)} = \tau_{vLC}\left(\frac{N_C}{10^4}\right)^{0.4\log\left(\frac{\tau_{vHC}}{\tau_{vLC}}\right)}$$

τ_{vHC} = permissible high cycle torsional vibration stress amplitude calculated according to the criteria in 4 but with a 6.25% lower safety factor and without the bending stress influence. For propeller shafts in way of and aft of the aft stern tube bearing the bending influence is covered by an increase of S by 0.05.

τ_{vLC} = permissible low cycle torsional vibration stress amplitude calculated according to the criteria in Sec.3 [2] a). For propeller shafts in way of and aft of the aft stern tube bearing the bending influence is covered by an increase of S by 0.05.

N_C = accumulated number of load cycles ($10^4 < N_C < 3 \cdot 10^6$). For determination of the relevant N_C, see the DNVGL-RU-SHIP Pt.4 Ch.2 Sec.2 [2.4.3], or a detailed method in [2.1].

2.1 The accumulated number of cycles, N_c

The accumulated number of cycles, N_c shall be based upon an equivalent number of cycles that results in the same accumulated partial damage (Miner's theory) as the real load spectrum. This means that each cycle with somewhat lower stress amplitudes will not be counted equally as one with the maximum amplitude, but will be "levelled" in proportion to the number of cycles to failure for the maximum amplitude. Since low amplitudes do not contribute to the damage sum, this is done in steps of 10% down to 60% of the maximum amplitude, see Figure 1 and Figure 2.

The procedure is as follows:

1) Record torsional vibrations, see Figure 1 and Figure 2.

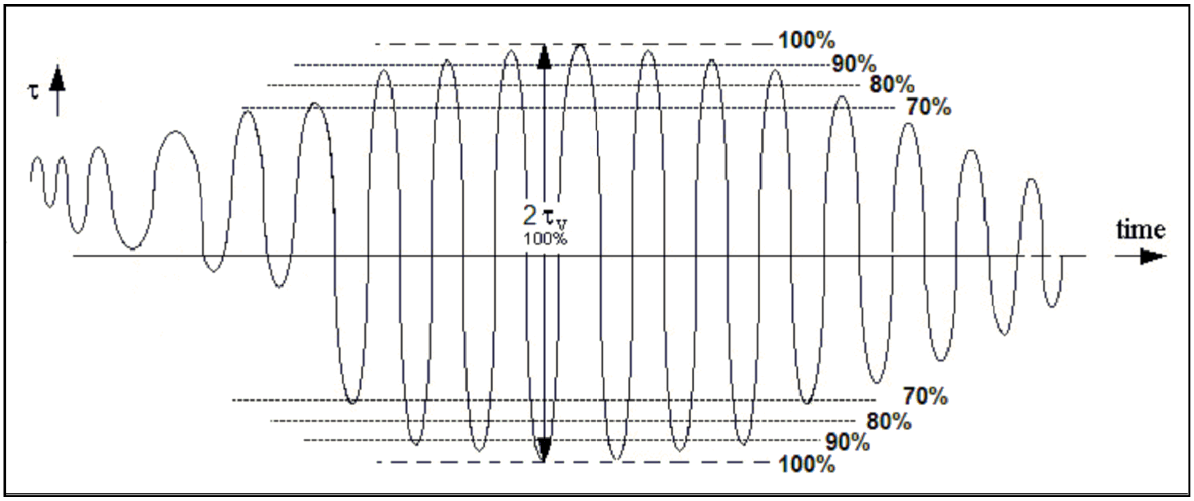

Figure 1 τ_v during stopping

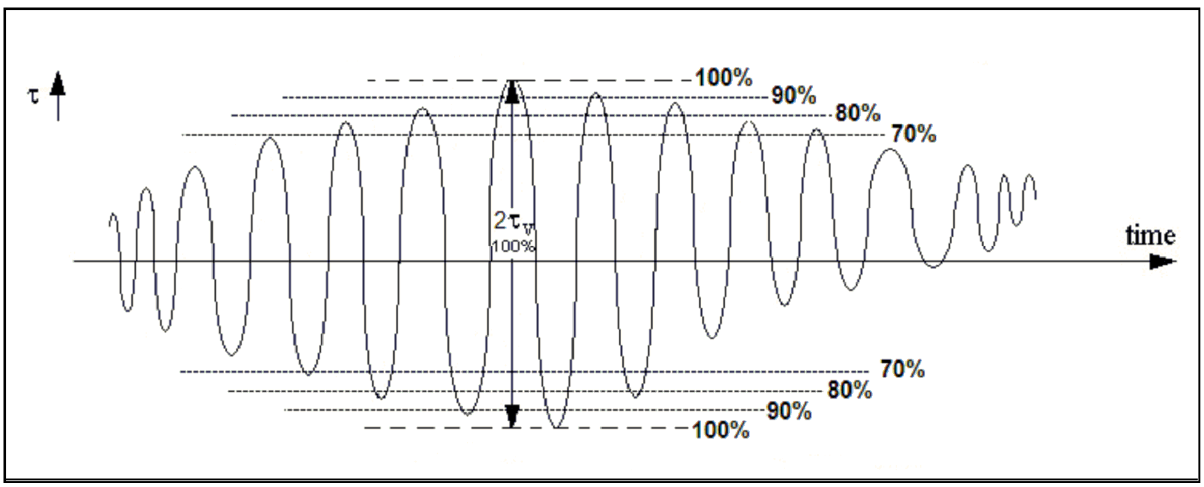

Figure 2 τ_v during starting

2) Determine the maximum double amplitude 2 τ_v considering both start and stop and use this as reference for 100%.

3) Draw lines in both start and stop records with double amplitude 100%, 90%, 80% and so on, see Figure 1 and Figure 2.

4) Count number of cycles N_{100} between 90% and 100%. This range will then be considered as amplitudes of 100%. Count number of cycles N_{90} between 80% and 90% (higher amplitudes shall not be counted again!). This range will then be considered as amplitudes of 90%, and so on.

5) Determine the double logarithmic τ-N curve by means of τ_{vLC} and τ_{vHC} calculated according to [2], see Figure 3.

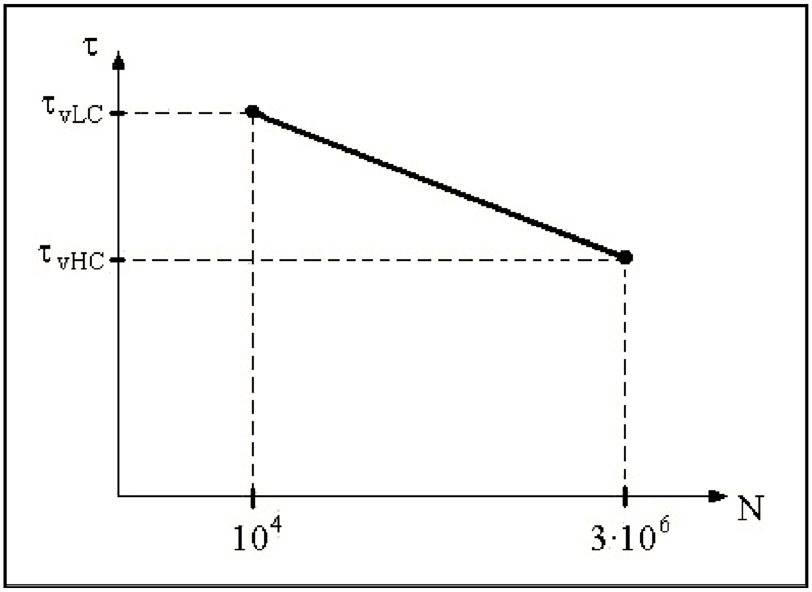

Figure 3 Double logarithmic τ-N curve

With this characteristic the equivalent number of cycles with 100% amplitude are calculated by means of division of the counted cycles with denominators determined as:

- 90% level with denominator $1.3^{\left(\frac{1}{\log\frac{\tau_{vLC}}{\tau_{vHC}}}\right)}$

- 80% level with denominator $1.7^{\left(\frac{1}{\log\frac{\tau_{vLC}}{\tau_{vHC}}}\right)}$

- 70% level with denominator $2.4^{\left(\frac{1}{\log\frac{\tau_{vLC}}{\tau_{vHC}}}\right)}$

6) Calculate the equivalent number of cycles for *one* passage up and down as:

$$N_e = N_{100} + \frac{N_{90}}{1.3^{\left(\frac{1}{\log\frac{\tau_{vLC}}{\tau_{vHC}}}\right)}} + \frac{N_{80}}{1.7^{\left(\frac{1}{\log\frac{\tau_{vLC}}{\tau_{vHC}}}\right)}} + \frac{N_{70}}{2.4^{\left(\frac{1}{\log\frac{\tau_{vLC}}{\tau_{vHC}}}\right)}}$$

7) Determine accumulated number of cycles N_c as N_e times number of passages, see 8).
8) The next question is; how many passages through the barred speed range (up and down together) shall be foreseen for the ship in question? The Society uses the following guidelines, if not otherwise is substantiated:

   — large carriers with fixed pitch propeller and manoeuvring speed below the barred speed range respectively with controllable pitch propeller. Once every week, resulting in a total of 1000 passages
   — large carriers with fixed pitch propeller and manoeuvring speed above the barred speed range. Five times every week, resulting in 5000 passages
   — vessels for short trade, once every day, resulting in 7000 passages
   — ferries for short distances, 20 times per day, resulting in 150 000 passages.

   Even though the above numbers are rough estimates one should bear in mind that logarithmic scales are used, so that a mistake by a factor of 2 or 3 on the number passages will have very little influence on the corresponding permissible stresses. It is more important to put effort in trying to estimate the number of load cycles for each passage correctly by simulation technique or measurements from similar plants in service.

SECTION 6 THE GEOMETRICAL STRESS CONCENTRATION FACTORS

1 Definition and general remarks

The stress concentration factors, α are defined:

— for bending as the ratio between the maximum principal stress and the nominal bending stress

— for torsion as the ratio between the maximum principal stress divided by $\sqrt{3}$ or the maximum shear stress (whichever is the highest) and the nominal torsional stress.

Stress concentration factors may be taken from well documented measurements, finite element calculations, recognised literature or from the formulae summarised in [2] to [10].

Only stress concentrations that are typical for shafting in marine applications are described here.

Note that these stress concentration factors are based on nominal stresses calculated by the minimum shaft diameter, d at the notch, and considering the influence of a central axial hole with diameter d_i. The reduction of the first moment of area due to keyway(s), longitudinal slot(s) or radial hole(s) is not considered.

It is recommended to design with generous fillet radii, in particular in areas where the checking of the radius may be difficult (e.g. keyways).

2 Shoulder fillets and flange fillets

The following stress concentration factors are valid for both shoulder fillets and flange fillets provided that the inner diameter d_i is less than 0.5d:

For shoulder fillets:

Higher stress concentration factors apply if a part is shrunk on to the bigger diameter, D of the shoulder as indicated in the last figure in [3]. This increase may be simplified by using a 10% larger value for D in the formulae in Table 1.

Table 1 Stress concentration factors, shoulder fillets and flange fillets

Design	*For low and high cycle fatigue*
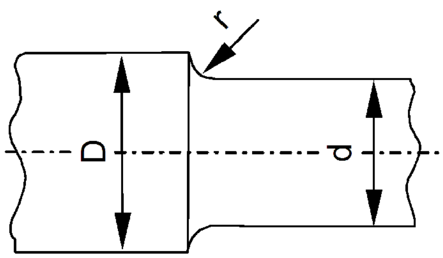	$$\alpha_b = 1 + \frac{1}{\sqrt{1.24\frac{r}{D-d} + 11.6\frac{r}{d}\left(1+2\frac{r}{d}\right)^2 + 1.6\frac{d}{D}\left(\frac{r}{D-d}\right)^3}}$$
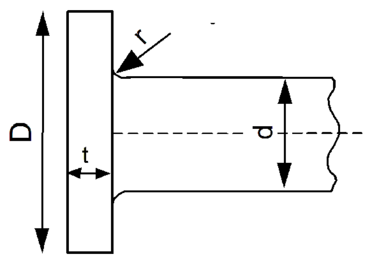	$$\alpha_t = 1 + \frac{1}{\sqrt{6.8\frac{r}{D-d} + 38\frac{r}{d}\left(1+2\frac{r}{d}\right)^2 + 4\frac{d}{D}\left(\frac{r}{D-d}\right)^2}}$$
	For combinations of small relative flange thicknesses (t/d) and small relative fillet radii (r/d) as e.g. $(r + t)/d < 0.35$ the α_t increases. This shall be taken into account by multiplying α_t with $1 + (0.08\ d/(r + t))^2$
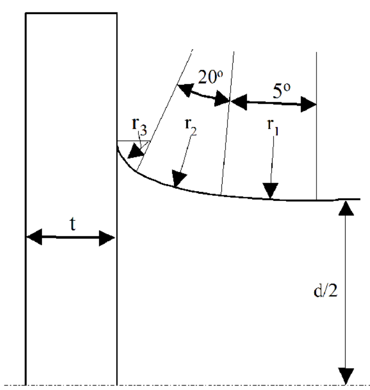	Multiradii transitions with flange thickness $t \geq 0.2\ d$: $\alpha_t \approx 1.05$ $\alpha_b \approx 1.1$ This may be obtained by e.g. starting with $r_1 = 2.5\ d$ tangentially to the shaft over a 5° sector, followed by $r_2 = 0.65\ d$ over 20° and finally $r_3 = 0.09\ d$ over 65°

3 U-Notch

The stress concentration factors in Table 2 are valid for U-notches (grooves), provided that the inner diameter, d_i is less than 0.5d.

Table 2 Stress concentration factors, U-notch

Design	*For low and high cycle fatigue*
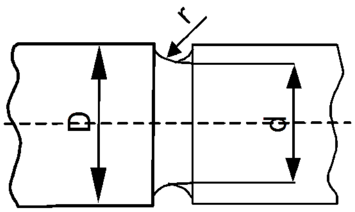	$\alpha_b = 1 + \dfrac{1}{\sqrt{0.4\dfrac{r}{D-d} + 5.5\dfrac{r}{d}\left(1+2\dfrac{r}{d}\right)^2}}$
	$\alpha_t = 1 + \dfrac{1}{\sqrt{1.4\dfrac{r}{D-d} + 20.6\dfrac{r}{d}\left(1+2\dfrac{r}{d}\right)^2}}$

4 Step with Undercut

Stress concentration for a step with undercut may be determined by interpolation between a shoulder fillet [2] and a U-notch [3], see Figure 1:

$$\alpha_b = \alpha_{b(6.2)} + (\alpha_{b(6.3)} - \alpha_{b(6.2)})\sqrt{\frac{d_1 - d}{D - d}}$$

$$\alpha_t = 1.04\ \alpha_{t(6.2)}$$

$\alpha_b(6.2)$ = stress concentration factor for a shoulder fillet, bending, see [2]

$\alpha_b(6.3)$ = stress concentration factor for a U-notch, bending, see [3]

$\alpha_t(6.2)$ = stress concentration for a shoulder fillet, torsion, see [2].

Dimensions, see Figure 1.

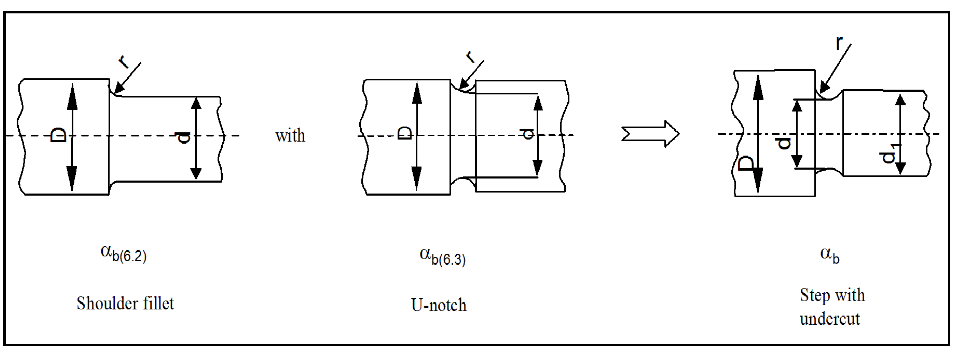

Figure 1 Stress concentration factors, step with undercut

5 Shrink fits

The stress concentration factors in Table 3 is valid for shrink fits. These factors mainly consider the risk for fretting and is therefore not considered as geometrical stress concentration factors.

Table 3 Stress concentration factors, shrink fits

<table>
<tr><td rowspan="2">Design</td><td>For low cycle fatigue</td><td colspan="2">For high cycle fatigue</td></tr>
<tr><td>α_t 1)</td><td>$\frac{\alpha_b}{m_b} = K_{H\sigma}$ 1)</td><td>$\frac{\alpha_t}{m_t} = K_{H\tau}$ 1)</td></tr>
<tr><td rowspan="3">Keyway(s)
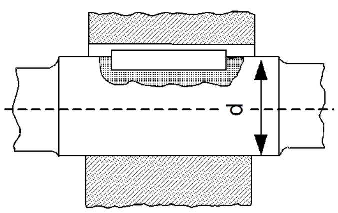</td><td rowspan="2">1.4</td><td>$1.4 + \frac{\sigma_B}{500}$</td><td>$0.9 + \frac{\sigma_B}{1000}$</td></tr>
<tr><td colspan="2">Two keyways
Due to reduction in the cross section area, the above values shall be increased by 15%</td></tr>
<tr><td colspan="3">The keyway(s) shall also be considered, see [6]</td></tr>
<tr><td>Keyless
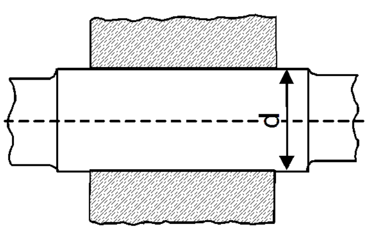</td><td>1.4</td><td>$1.05 + \frac{\sigma_B}{500}$</td><td>$0.71 + \frac{1.2\ \sigma_B}{1000}$</td></tr>
<tr><td>With relief
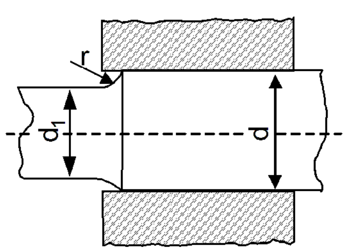</td><td colspan="3">For designs with suitable relief grooves or shoulder steps at the end of the hub, the stress concentration may be considerably reduced, even close to unity if d = 1.1d_1 and r = 2 (d-d_1) and an axial overshoot near zero but not less than zero. This is valid only if no relative micro-movement between the 2 parts can be verified; see the DNVGL-RU-SHIP Pt.4 Ch.4 Sec.1 [2.4.2] regarding surface pressure. However, the groove or shoulder itself shall be calculated as such.</td></tr>
<tr><td colspan="4">1) These notch factors also contain the influence of typical surface roughness and size influence. Hence the surface roughness terms and size influence term in the component influence factors shall be disregarded.</td></tr>
</table>

For hollow shafts with a relatively large inner diameter the notch factors are higher. However, this can be compensated by means of an expansion sleeve in the inner bore.

6 Keyways

The stress concentration factors in the bottom of a keyway are given in Table 4.

Table 4 Stress concentration factors, keyways

Design	*For low and high cycle fatigue*
Semicircular ends 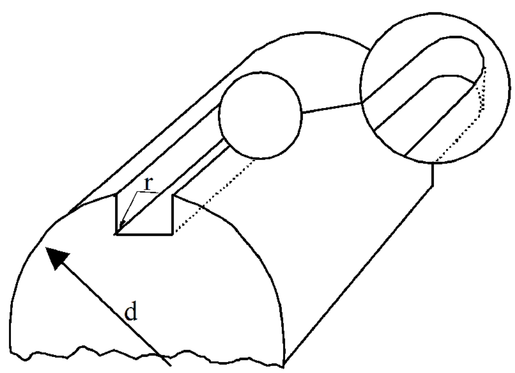 	$\alpha_b = 1.4 + 0.015 \frac{d}{r}$ (for $\frac{r}{d} < 0.006$ this formula gives too high stress concentration)
	$\alpha_t = 2.1 + 0.012 \frac{d}{r}$ (for $\frac{r}{d} < 0.0075$ this formula gives too high stress concentration)
Sled runner ends 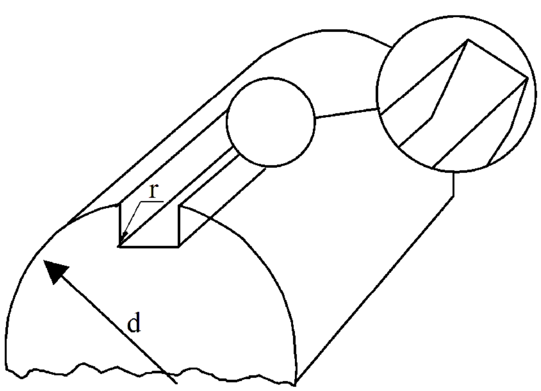 	$\alpha_b = 1.4$
	$\alpha_t = 2.1 + 0.012 \frac{d}{r}$ (for (r/d) < 0.0075 this formula gives too high stress concentration)

For hollow shafts with inner diameter greater than 0.5 d, the increase of nominal stresses due to the keyway(s) shall be considered.

Note that these stress concentration factors shall be used together with the real nominal stresses applied at the end of the keyway, see Figure 2, i.e. the influence of hub stiffening in bending and torque transmission due to friction may be considered.

The shrink fit between shaft and hub shall also be considered, see [5].

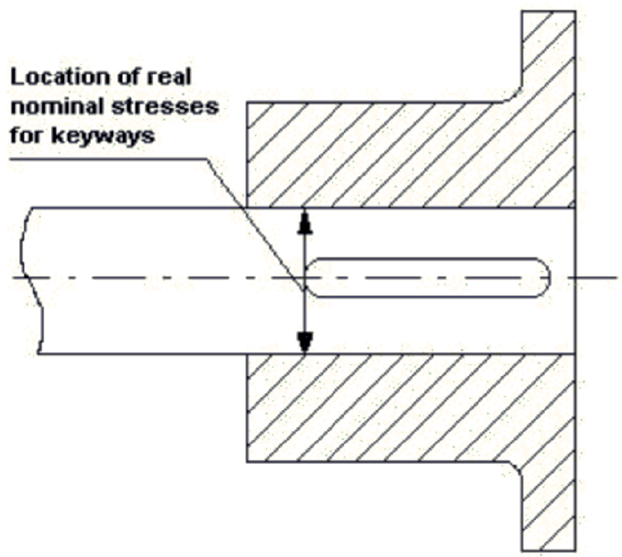

Figure 2 Keyway Inside Hub

7 Radial holes

For a radial hole with diameter $d_h < 0.2 \cdot d$ and a central bore $d_i < 0.5 \cdot d$ (i.e. 2 outlet holes diametrically opposed), the stress concentration factors at the surface in the radial hole outlets are:

Table 5 Stress concentration factors, radial holes

Design	*For low and high cycle fatigue*
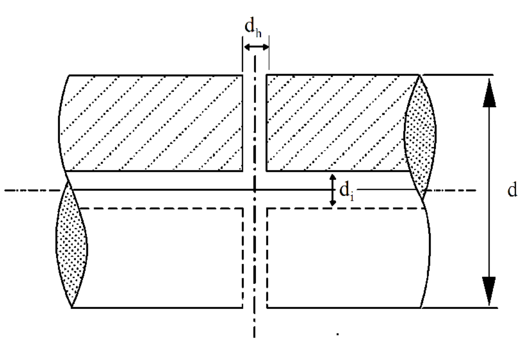	$\alpha_b = 3 - 5.9\frac{d_h}{d} + 34.6\left(\frac{d_h}{d}\right)^2$
	$\alpha_t = 2.3 - 3\frac{d_h}{d} + 15\left(\frac{d_h}{d}\right)^2 + 10\left(\frac{d_h}{d}\right)^2\left(\frac{d_i}{d}\right)^2$ or simplified to: $\alpha_t = 2.3$
As an approximation the same formulae may be used if only one outlet.	

Design	*For low and high cycle fatigue*
With intersecting eccentric axial bore 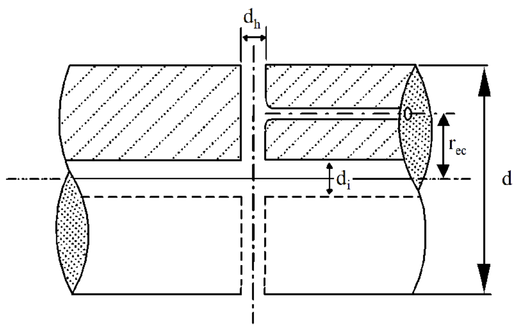	Multiply the above formulae with: $$1 + k_{ec}^4$$ $$k_{ec} - \text{eccentricity ratio} = \frac{2r_{ec}}{d}$$ — For k_{ec} > 0,85 the stress concentration will be specially considered.

The notch radius to be used in the formulae for component influence factors in Sec.4 [4] is the radial hole radius = $d_h/2$ and the nominal stress is based on the full section.

Note:

The stress concentration in the intersection itself can be much higher and is subject to special consideration. For plants with high torsional vibrations, such as direct coupled plants, no sharp edges are acceptable.

---e-n-d---o-f---n-o-t-e---

8 Longitudinal slot

For longitudinal slots, the stress concentration factor is given in Table 6.

Table 6 Stress concentration factors, longitudinal slots

Design	*For low and high cycle fatigue*
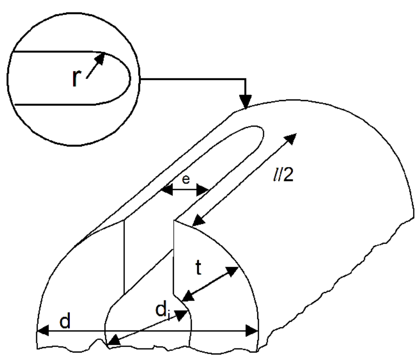	$$\alpha_t = \alpha_{t(6.5)} + 0.8\,\frac{(l-e)/d}{\sqrt{\left[(1-\frac{di}{d}) \times \frac{e}{d}\right]}}$$ $\alpha_{t(6.5)}$ = stress concentration factor for a radial hole with d_h = e, in torsion, see [5]. The formula is valid for: — for outlets each 180 degrees and for outlets each 120°C — slots with semicircular ends, i.e. r = e/2. A multi-radii slot end can reduce the local stresses. — no edge rounding (except chamfering), as any edge rounding increases the α_t slightly.

The radius to be used in the formulae for component influence factors in Sec.4 [4] is e/2.

9 Splines

The stress concentration factors[1)] given in Table 7 may be applied.

Table 7 Stress concentration factors, splines

Design	*For low cycle fatigue*	*For high cycle fatigue*	
	α_t 2)	$\frac{\alpha_b}{m_b} = K_{H\sigma}$ 2)	$\frac{\alpha_t}{m_t} = K_{H\tau}$ 2)
Involute splines: 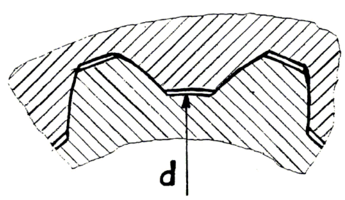 	1.15	$0.96+\frac{\sigma_y}{1000}$	$0.92+\frac{\sigma_y}{1500}$
Non-involute splines: 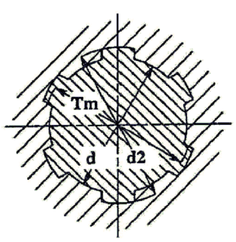 Parallell splines 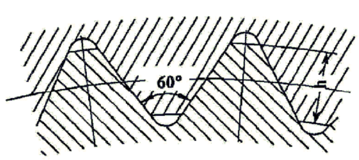 Trapezodial (serrated) splines	Higher notch factors apply (10%)		

1) Note that the nominal stresses are based on the root diameter of the splines.
2) These notch factors also contain the influence of typical surface roughness and size influence. Hence the surface roughness terms and size influence term in the component influence factors shall be disregarded.

Surface hardened splines are subject to special consideration, see Sec.3 [6] and Sec.4 [5].

Note that higher notch factors apply if the hub is very rigid, i.e. the torque transmission is concentrated at the hub edge, see Figure 3.

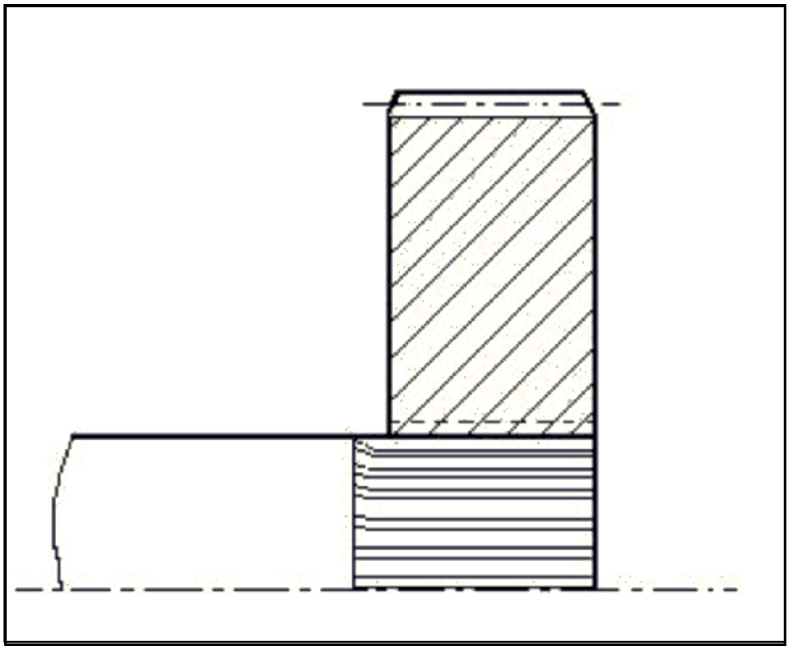

Figure 3 Spline connection with very rigid hub

10 Square groove (circlip)

The stress concentration factors given in Table 8 may be applied.

Table 8 Stress concentration factors, square grove (circlip)

<table>
<tr><td rowspan="2">Design</td><td>For low cycle fatigue</td><td colspan="2">For high cycle fatigue</td></tr>
<tr><td>α_t</td><td>α_b/m_b</td><td>α_t/m_t</td></tr>
<tr><td rowspan="2">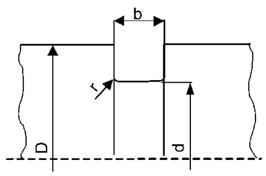</td><td rowspan="2">3.0</td><td>$1.03+\sqrt{\frac{0.4724(D-d)}{r+2.9\cdot 10^{-(0.514+0.00152\sigma_y)}}}$</td><td>$1.48+\sqrt{\frac{0.1013(D-d)}{r+10^{-(0.514+0.00152\sigma_y)}}}$</td></tr>
<tr><td colspan="2">Other standards as e.g. DIN 743 indicate upper limits as 4 respectively 2.5. These recommendations are probably based on fatigue test result, but without having checked the likely influence of compressive residual stresses from machining. Residual stresses in sharp notches can have a strong influence, and it is risky to rely on upper limits for such notches.
— If $\frac{2b}{D-d} < 1.4$, multiply the above formulae with: $0.94\left(\frac{b}{D-d}\right)^{-0.2}$</td></tr>
</table>

APPENDIX A EXAMPLES

The examples presented in this appendix are solely meant for demonstration of the calculation method and shall not be used for dimensioning purposes as fictitious loads and dimensions are used.

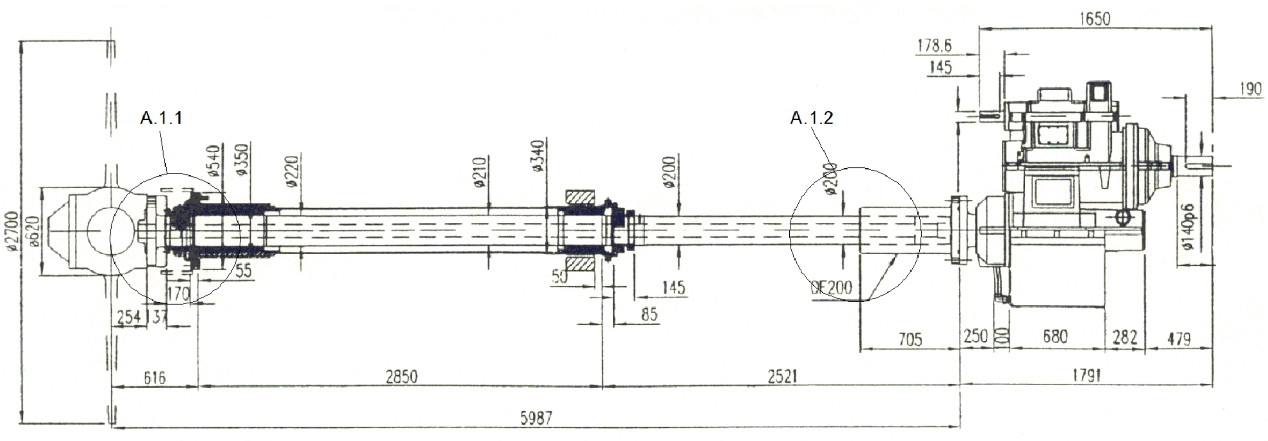

Figure 1 Geared CP-propeller plant

1 Calculation example 1: Propeller shaft in a geared, controllable pitch plant with no ice-class

The shaft arrangement is shown in Figure 1.

1.1 In way of propeller flange

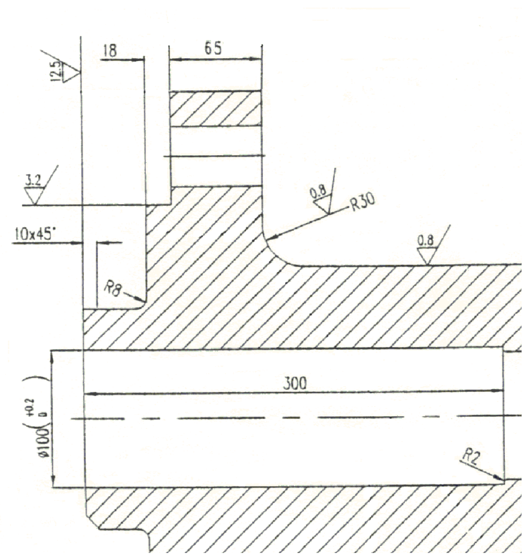

Figure 2 Propeller flange fillet

Relevant loads:

— torque at maximum continuous power, T_0 = 62 kNm
— application factors, repetitive cyclic torques (taken from the torsional vibration calculations):
— in normal operation condition, $K_{Anorm.}$ = 1.2
— in misfiring condition, $K_{Amisf.}$ = 1.3
— rotating bending moment, M_b = 24.8 kNm (taken from the shaft alignment calculations including the bending moment due to thrust eccentricity or as a simple and conservative estimation by $0.4T_0$)
— no significant clutching-in shock loads.

Relevant dimensions:

— outer diameter, d = 220 mm
— inner diameter, d_i = 100 mm
— flange diameter, D = 475 mm
— radius of flange fillet, r = 30 mm
— flange thickness, t = 65 mm
— surface roughness in flange fillet, R_a = 0.8 μm,
 i.e. $R_y \approx$ 4.8 μm.

Relevant material data:

— EN 10083-1: C45E +N (1.1191) with the following mechanical properties for representative test pieces[4]:
— ultimate tensile strength, $\sigma_B \geq$ 560 N/mm^2
— yield strength, $\sigma_y \geq$ 275 N/mm^2.

Calculations:

The low cycle criterion (see Sec.3 [2]):

$$\tau_{max} = \tau_0 K_A \leq \frac{\sigma_y}{2\,S\,K_L}$$

— nominal torsional stress at maximum continuous power (see Sec.3 [3]):

$$\tau_0 = \frac{16 \cdot 220 \cdot 62 \cdot 10^6}{\pi(220^4 - 100^4)}\ \mathrm{N/mm^2} = 30.98\ \mathrm{N/mm^2}$$

— application factor (maximum K_A to be used in this criterion, see Sec.3 [3]):
 $K_{Amisf.}$ = 1.3
— yield strength:
 σ_y = 275 N/mm^2
— safety factor (see the DNVGL-RU-SHIP Pt.4 Ch.4 Sec.1 [2.2.3]):
 S = 1.25
— geometrical stress concentration factor, torsion (see Sec.6 [2]):
 α_t = 1.33
— component influence factor for low cycle fatigue (see Sec.3 [5]):

$$K_L = 1 + (1.33 - 1)\frac{275}{900} + 10^{-4}(560 - 200)\log 4.8 = 1.13$$

[4] DNVGL-RU-SHIP Pt.2 Ch.2 Sec.6.

Consequently:

$$1.3 \cdot 30.98\ \mathrm{N/mm^2} \leq \frac{275}{2 \cdot 1.25 \cdot 1.13}\ \mathrm{N/mm^2}$$

$$\Updownarrow$$

$$40.3\ \mathrm{N/mm^2} \leq 97.3\ \mathrm{N/mm^2}$$

or actual safety factor, S = 3.0

Conclusion: Criterion fulfilled.

The high cycle criterion (see Sec.4 [2]):

$$\left(\frac{\tau_v}{\tau_f}\right)^2 + \left(\frac{\sigma_b}{\sigma_f}\right)^2 \leq \frac{1}{S^2}$$

— nominal vibratory torsional stress for continuous operation (see Sec.4 [2]):

$\tau_v = (K_{Anorm.} - 1)\tau_0 = (1.2 - 1)\ 30.98\ \mathrm{N/mm^2}$
$= 6.20\ \mathrm{N/mm^2}$

— nominal reversed bending stress amplitude:

$$\sigma_b = \frac{32 \cdot 220 \cdot 24.8 \cdot 10^6}{\pi(220^4 - 100^4)}\ \mathrm{N/mm^2} = 24.8\ \mathrm{N/mm^2}$$

— geometrical stress concentration factors (see Sec.6 [2]):

torsion: $\alpha_t = 1.33$

bending: $\alpha_b = 1.61$

— notch sensitivity coefficients (see Sec.4 [4.1]):

$$\text{Torsion: } m_t = 1 + \left(\frac{60}{275} - 0.05\right)\sqrt{\frac{1}{30}} = 1.03$$

$$\text{Bending: } m_b = 1 + \left(\frac{60}{275} - 0.05\right)\sqrt{\frac{2}{30}} = 1.04$$

— component influence factors for high cycle fatigue (see Sec.4 [4]):

$$\text{Torsion: } K_{H\tau} = \frac{1.33}{1.03} + 0.01\sqrt{30} + 3 \cdot 10^{-4}(560 - 200)\log 4.8 = 1.42$$

$$\text{Bending: } K_{H\sigma} = \frac{1.61}{1.04} + 0.01\sqrt{30} + 4 \cdot 10^{-4}(560 - 200)\log 4.8 = 1.70$$

— high cycle fatigue strengths (see Sec.4 [3]):

$$\text{Torsion: } \tau_f = \frac{0.24 \cdot 275 + 42 - 0.15 \cdot 30.98}{1.42} = 72.78 \text{ N/mm}^2$$

$$\text{Bending: } \sigma_f = \frac{0.4 \cdot 275 + 70 - 0.4 \cdot 30.98}{1.70} = 98.59 \text{ N/mm}^2$$

— safety factor (see DNVGL-RU-SHIP Pt.4 Ch.4 Sec.1 [2.2.3]): S = 1.6

Consequently:

$$\left(\frac{6.20}{72.78}\right)^2 + \left(\frac{24.78}{98.59}\right)^2 = 0.07 \le \left(\frac{1}{1.6}\right)^2 = 0.39$$

or actual safety factor, S = 3.8

Conclusion: Acceptable, and the dimensions could be reduced provided that the stern tube bearing pressure remains within the acceptable rule limits in all operating conditions (full and idle speed respectively).

The transient vibration criterion (see Sec.5):

Not applicable since this is a geared plant with no barred speed range.

1.2 In way of shaft coupling

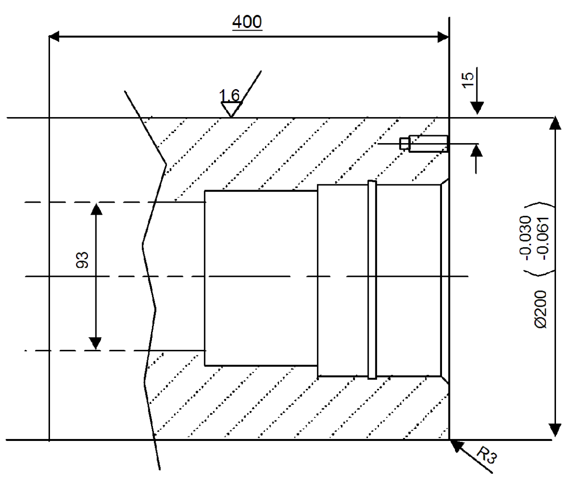

Figure 3 Propeller shaft end at shrink fit coupling

Relevant loads:

— torque at maximum continuous power, T_0 = 62 kNm
— application factors, repetitive cyclic torques (taken from the torsional vibration calculations):
in normal operation condition, $K_{Anorm.}$ = 1.2
in misfiring condition, $K_{Amisf.}$ = 1.3
— negligible rotating bending moment (confirmed by shaft alignment analysis)
— no significant clutching-in shock loads.

Relevant dimensions:

— outer diameter, d = 200 mm
— inner diameter, d_i = 93 mm
— surface roughness, R_a = 1.6 μm, i.e. $R_y \approx$ 9.6 μm.

Relevant material data:

EN 10083-1: C45E + N (1.1191) with the following mechanical properties for representative test pieces [5]:

Ultimate tensile strength, $\sigma_B \geq$ 560 N/mm^2.

Yield strength, $\sigma_y \geq$ 275 N/mm

Calculations:

The low cycle criterion (see Sec.3 [2]):

$$\tau_{max} = \tau_0 K_A \leq \frac{\sigma_y}{2\,S\,K_L}$$

— nominal torsional stress at maximum continuous power (see Sec.3 [3]):

$$\tau_0 = \frac{16 \cdot 200 \cdot 62 \cdot 10^6}{\pi(200^4 - 93^4)} \text{ N/mm}^2 = 41.41 \text{ N/mm}^2$$

— application factor (maximum K_A to be used in this criterion, see Sec.3 [3]):
$K_{Amisf.}$ = 1.3
— yield strength:
σ_y = 275 N/mm^2
— safety factor (see DNVGL-RU-SHIP Pt.4 Ch.4 Sec.1 [2.2.3]):
S = 1.25
— geometrical stress concentration factor, torsion (see Sec.6 [5]):
α_t= 1.4
— component influence factor for low cycle fatigue (see Sec.3 [5]):

$$K_L = 1 + (1.4 - 1)\frac{275}{900} = 1.12$$

[5] See DNVGL-RU-SHIP Pt.2 Ch.2 Sec.6

Consequently:

$$1.3 \cdot 41.41\,\text{N/mm}^2 \le \frac{275}{2 \cdot 1.25 \cdot 1.12}\,\text{N/mm}^2$$
$$\Updownarrow$$
$$53.8\,\text{N/mm}^2 = 98.2\,\text{N/mm}^2$$

or actual safety factor, S = 2.3.

Conclusion: Criterion fulfilled.

The high cycle criterion (see Sec.4 [2]):

$$\left(\frac{\tau_v}{\tau_f}\right) + \left(\frac{\sigma_b}{\sigma_f}\right) \le \frac{1}{S^2}$$

— nominal vibratory torsional stress for continuous operation (see Sec.4 [2]):

τ_v = $(K_{Anorm.} - 1)\tau_0$ = (1.2 - 1) 41.41 N/mm^2
= 8.28 N/mm^2

— geometrical stress concentration factor, torsion (see Sec.6 [5]):

$$\frac{\alpha_t}{m_t} = 0.71 + \frac{1.2 \cdot 560}{1000} = 1.38$$

— this notch factor contains also the influence of the surface roughness and size influence. Hence, the component influence factor for high cycle torsional fatigue (see Sec.4 [4]):

$K_{H\tau}$ = 1.38

— high cycle torsional fatigue strength (see Sec.4 [3]):

$$\text{Torsion: } \tau_f = \frac{0.24 \cdot 275 + 42 - 0.15 \cdot 41.41}{1.38}\,\text{N/mm}^2$$
$$= 73.76\,\text{N/mm}^2$$

— $(\sigma_b / \sigma_f)^2 \approx 0$, since rotating bending moment is negligible at this section of the shaft

— safety factor (see DNVGL-RU-SHIP Pt.4 Ch.4 Sec.1 [2.2.3]):

S = 1.6

Consequently:

$$\left(\frac{8.28}{73.76}\right) = 0.013 \le \left(\frac{1}{1.6}\right)^2 = 0.39$$

for actual safety factor, S = 8.8

Conclusion: Acceptable, and it means that the shaft dimensions may be reduced, provided that acceptable friction torque transmission through the shrink fit coupling is maintained.

The transient vibration criterion (see Sec.5):

Not applicable since this is a geared plant with no barred speed ranges.

2 Calculation example 2: Oil distribution shaft in a direct coupled, controllable pitch propeller plant with no ice-class:

The shaft arrangement is shown in Figure 4.

Main engine: 6 cylinder MAN B&W 6S42MC rated to 5300 kW at 120 r.p.m.

Control system: Only pitch control, i.e engine running at constant speed. No combinator mode.

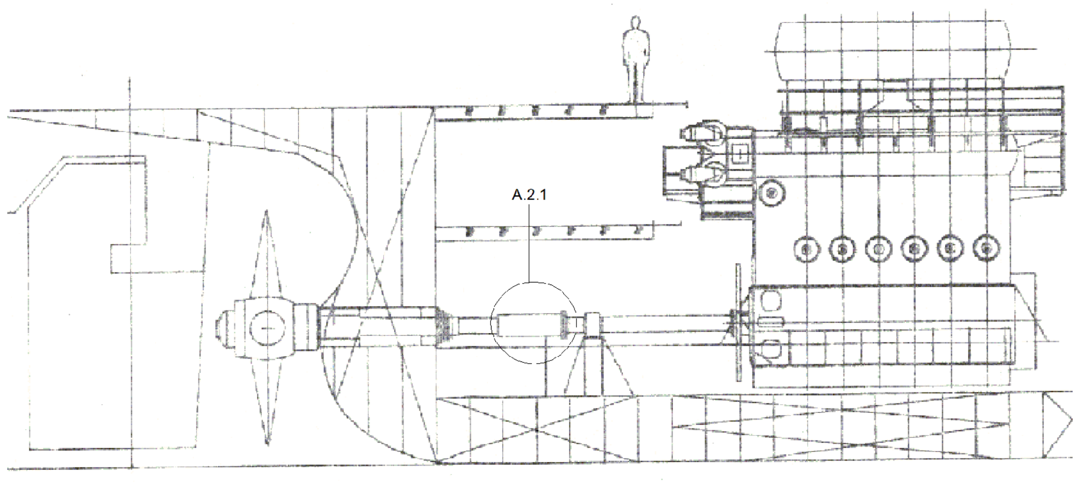

Figure 4 Direct coupled CP-propeller plant

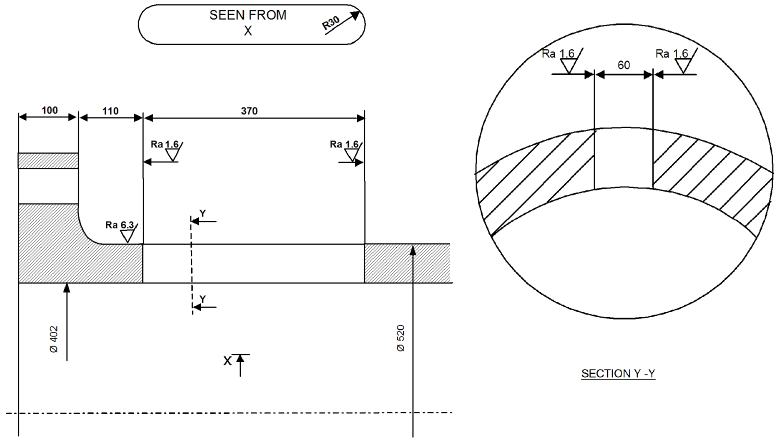

Figure 5 Design of slot in O.D.-shaft

2.1 In way of slot in the oil distribution shaft:

Relevant loads:

— torque at maximum continuous power, T_0 = 421.8 kNm at n_0 = 120 r.p.m.
— negligible rotating bending moment (confirmed by shaft alignment analysis)
— calculated steady state torsional vibrations (full pitch) according to Figure 6.

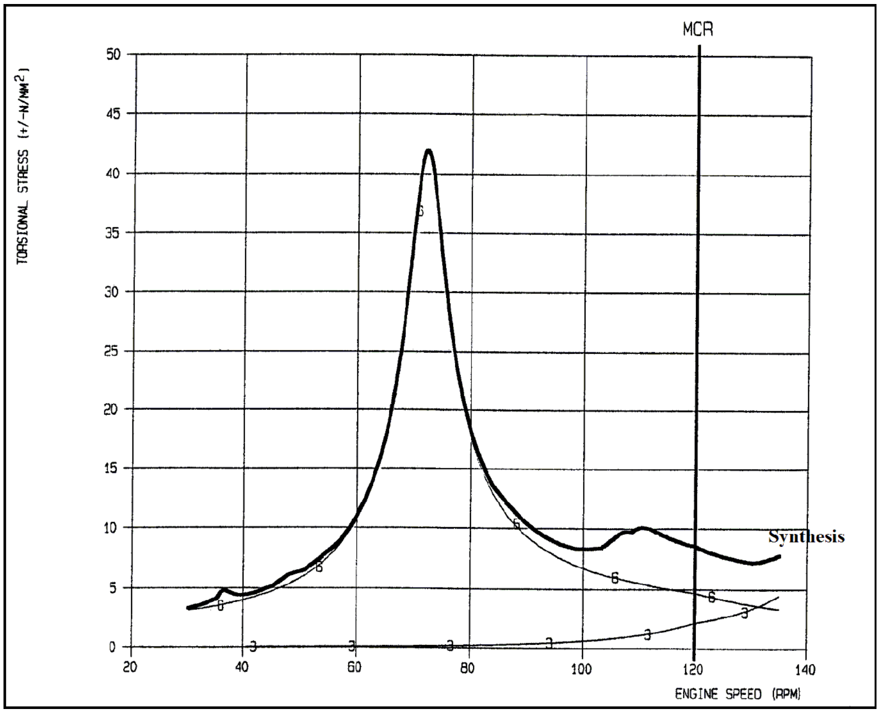

Figure 6 Torsional vibration calculations in normal condition with full pitch

In this case the calculated torsional vibration level for zero pitch reaches approximately the same level as for full pitch, see Figure 9. The reason for this is that both the engine excitation and propeller damping is lower for zero pitch than for full pitch. The 6^{th} order resonance speed is 72 r.p.m. (1. mode natural frequency = 433.6 vibr/min) for full pitch and 74 r.p.m. for zero pitch (1. mode natural frequency = 444 vibration/min.). In misfiring condition, the torsional vibration stresses due to the 6^{th} order excitation will be lower than for normal condition, due to one cylinder with no ignition, see Figure 7.

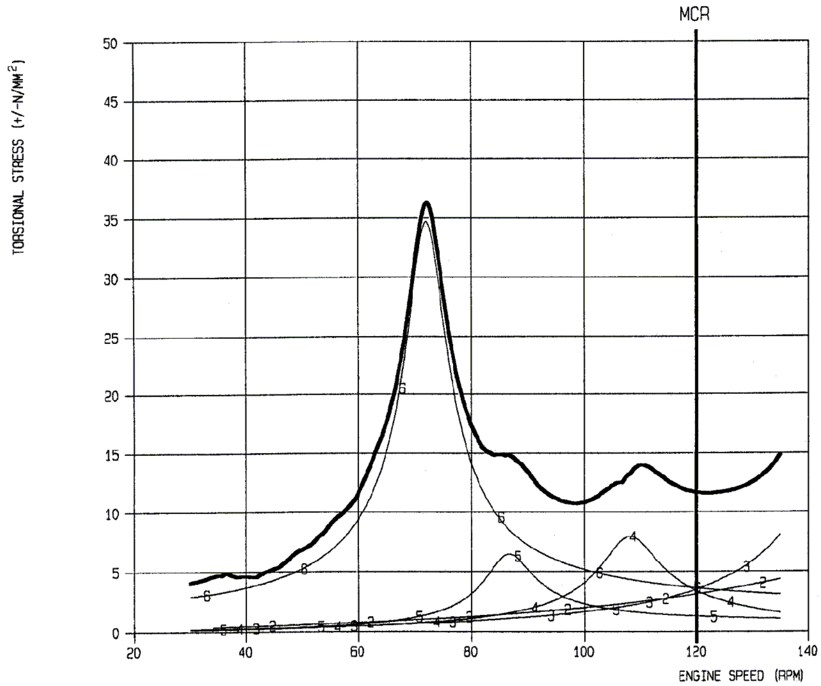

Figure 7 Torsional vibration calculations in misfiring condition with reduced pitch corresponding to 3500 kW at 120 r.p.m.

Relevant dimensions:

— number of slots: 3 (each 120°)
— outer diameter, d = 520 mm
— inner diameter, d_i = 402 mm
— length of slot, l = 370 mm
— width of slot, e = 60 mm
— surface roughness at the edge of the slot, R_a = 1.6 μm, i.e. $R_y \approx 9.6$ μm

Relevant material data:

— EN 10083-1: 42CrMo4 +QT (1.7225) with the following mechanical properties as specified by the designer for representative test pieces[6]:
ultimate tensile strength, $\sigma_B \geq 750$ N/mm^2
yield strength, $\sigma_y \geq 450$ N/mm^2

Calculations:

The low cycle criteria (see Sec.3 [2]):

a) Peak stress:

$$\tau_{max} = (\tau + \tau_v)_{max} \leq \frac{\sigma_y}{2\ S\ K_L}$$

6 See DNVGL-RU-SHIP Pt.2 Ch.2 Sec.6.

— nominal torsional stress at maximum continuous power (see Sec.3 [3]):

$$\tau_0 = \frac{16 \cdot 520 \cdot 421.8 \cdot 10^6}{\pi(520^4 - 402^4)} N/mm^2 = 23.77 \ N/mm^2$$

— maximum value of $(\tau + \tau_v)$ in the entire speed range (see Sec.3 [3]):

in this case there are three potential maximum values of $(\tau + \tau_v)$:

i) running with full pitch at n_0 = 120 r.p.m. in normal condition:

nominal torsional stress: τ_0 = 23.77 N/mm^2 and vibratory torsional stress (see Figure 6):

τ_v = 8.6 N/mm^2.

thus, in this case $(\tau + \tau_v)$ = 32.4 N/mm^2.

ii) running with full pitch at n_0 = 120 r.p.m in misfiring condition (one cylinder without combustion): since the thermal load on the remaining 5 cylinders will be too high at 120 r.p.m, the power (by pitch reduction) shall be reduced to 3500 kW. Nominal torsional stress at 120 r.p.m is then:

$$\tau_{0misf.} = \frac{3500}{5300} \cdot 23.77 \ N/mm^2 = 15.70 \ N/mm^2$$

vibratory torsional stress at 120 r.p.m in misfiring condition is according to the torsional vibration calculations: $\tau_{v\ misf.}$ = 11.7 N/mm^2. Thus, in this case $(\tau + \tau_v)$ = 27.4 N/mm^2.

iii) running (accidentally[7]) at 6th order resonance speed = 74 r.p.m with 0-pitch:

nominal torsional stress at 74 r.p.m with 0-pitch is assumed to be approximately 15% of the nominal torsional stress with full pitch:

$$\tau_{74r.p.m.} = 0.15\left(\frac{74}{120}\right)^2 23.77 \ N/mm^2 = 1.36 \ N/mm^2$$

vibratory torsional stress at 74 r.p.m with 0-pitch is according to the torsional vibration calculations (see Figure 9):

$$\tau_{v74r.p.m.} = 40.0 \ N/mm^2.$$

thus, in this case $(\tau + \tau_v)$ = 41.36 N/mm^2.

the maximum torsional stress occurs in case iii):

$$(\tau + \tau_v)_{max} = (\tau + \tau_v)_{74r.p.m} = 41.36 \ N/mm^2$$

— yield strength: σ_y = 450 N/mm^2

[7] Accidentally, since running steady at 74 r.p.m is not relevant as the high cycle criterion below concludes with a barred speed range around 74 r.p.m.

- safety factor (see DNVGL-RU-SHIP Pt.4 Ch.4 Sec.1 [2.2.3]): S = 1.25
- geometrical stress concentration factor, torsion (see Sec.6 [8]): α_t = 4.33
- component influence factor for low cycle fatigue (see Sec.3 [5]):

$$K_L = 1 + (4.33 - 1)\frac{450}{900} + 10^{-4}(750 - 200)\log 9.6 = 2.72$$

Consequently:

$$41.36\ \text{N/mm}^2 \leq \frac{450}{2 \cdot 1.25 \cdot 2.72}\text{N/mm}^2 = 66.2\ \text{N/mm}^2$$

or actual safety factor, S = 2.0

Conclusion: Criterion fulfilled.

b) Torque reversal:

$$\alpha_t \Delta\tau = \alpha_t(\tau_{max} + |\tau_{max\ reversed}|) \leq \frac{2\sigma_y}{S\sqrt{3}}$$

- the repetitive nominal stress range (see Sec.3 [4]):
  forward peak torsional stress, see criterion a):

$$\tau_{max} = 41.3\text{N/mm}^2$$

maximum reversed torsional stress:

$$|\tau_{max\ reversed}| = 40 - 1.28\ \text{N/mm}^2 = 38.7\ \text{N/mm}^2$$

thus,

$$\Delta\tau = 41.3 + 38.7\ \text{N/mm}^2 = 80\ \text{N/mm}^2$$

- safety factor (see DNVGL-RU-SHIP Pt.4 Ch.4 Sec.1 [2.2.3]):
  S = 1.25

Consequently:

$$4.33 \cdot 80\ \text{N/mm}^2 = 346.4\ \text{N/mm}^2 \leq \frac{2 \cdot 450}{1.25 \cdot \sqrt{3}}\ \text{N/mm}^2 = 415.6\ \text{N/mm}^2$$

or actual safety factor, S = 1.5.

Conclusion: Criterion fulfilled even when running (accidentally) at 74 r.p.m. with 0-pitch as discussed in criterion a) (running steady state at 74 r.p.m. is not relevant). The actual repetitive nominal stress range when passing quickly through the barred speed range will be lower, 33 N/mm^2 according to the measurements, see Figure 10. So the actual safety factor is even higher than 1.5.

The high cycle criterion (see Sec.4 [2]):

$$\left(\frac{\tau_v}{\tau_f}\right)^2 + \left(\frac{\sigma_b}{\sigma_f}\right)^2 \le \frac{1}{S^2}$$

— notch sensitivity coefficient for high cycle torsional fatigue (see Sec.4 [4.1]):

$$m_t = 1 + \left(\frac{60}{450} - 0.05\right)\sqrt{\frac{1}{30}} = 1.02$$

— component influence factor for high cycle torsional fatigue (see Sec.4 [4]):

$$K_{H\tau} = \frac{4.33}{1.02} + 0.01\sqrt{30} + 3 \cdot 10^{-4}(750 - 200)\log 9.6 = 4.46$$

— high cycle torsional fatigue strength (see Sec.4 [3]):

$$\tau_f = \frac{0.24 \cdot 450 + 42 - 0.15 \cdot 0.15 \cdot \lambda^2 \cdot 23.77}{4.46} \text{ N/mm}^2$$

$$= 33.6 - 0.12\lambda^2 \text{ N/mm}^2$$

λ is the speed ratio = n/n_0

— $\left(\frac{\sigma_b}{\sigma_f}\right)^2 \approx 0$ since rotating bending moment is negligible at this section of the shaft

— safety factor (see DNVGL-RU-SHIP Pt.4 Ch.4 Sec.1 [2.2.3]):
S = 1.6

Consequently:

The permissible torsional vibratory stress as a function of shaft speed is then:

$$\tau_{vHC} \le \frac{33.6 - 0.12\lambda^2}{1.6} \text{ N/mm}^2 = 21.0 - 0.075\lambda^2 \text{ N/mm}^2$$

This is then plotted as a function of engine speed in the calculated torsional vibration diagram, see Figure 8.

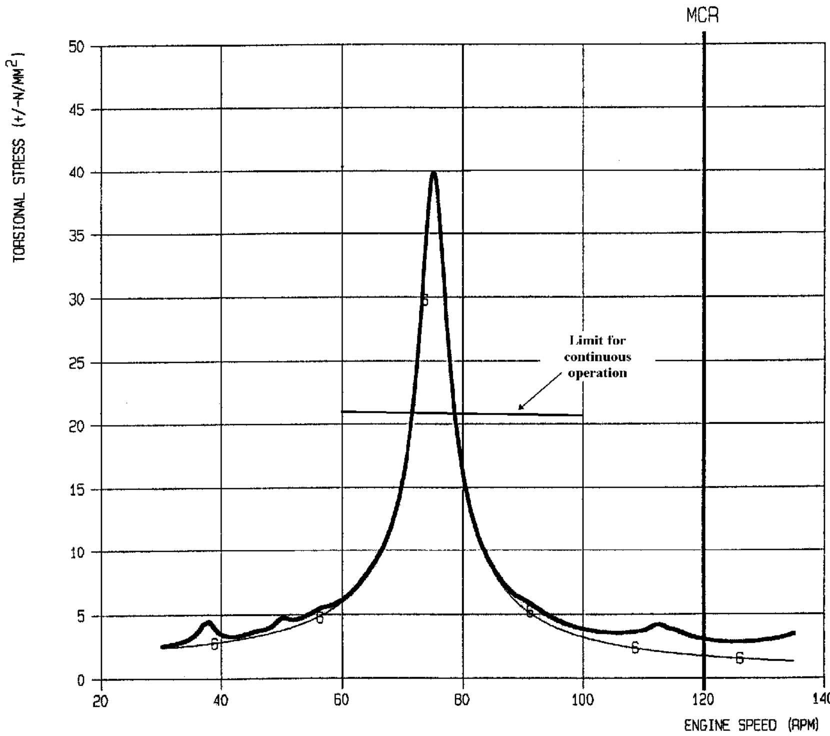

Figure 8 Calculated steady state torsional vibration stress and stress limit for continuous operation

Conclusion: The calculated stresses are higher than the allowable stresses for continuous operation around the 6th order resonance at 74 r.p.m. This means that a barred speed range shall be introduced from 67 to 79 r.p.m. In order to take into account some speed hunting and the inaccuracies of the calculations and engine tachometer, the barred speed range should be extended some r.p.m. (~ 2%). In this case the barred speed range should be set to 65 to 81 r.p.m. However, this shall be finally confirmed by torsional vibration measurements on board during the sea trials.

The transient vibration criterion (see Sec.5):

$$\tau_{vT} \le \tau_{vHC}\left(\frac{3 \cdot 10^6}{N_C}\right)^{0.4\log\left(\frac{\tau_{vLC}}{\tau_{vHC}}\right)} = \tau_{vLC}\left(\frac{N_C}{10^4}\right)^{0.4\log\left(\frac{\tau_{vHC}}{\tau_{vLC}}\right)}$$

— permissible high cycle torsional vibration stress, τ_{vHC}, as calculated above but with a safety factor of 1.5:

$$\tau_{vHC} = \frac{33.6 - 0.12\lambda^2}{1.5}\,\text{N/mm}^2 = 23.4 - 0.08\,\lambda^2\ \ \text{N/mm}^2$$

λ is the speed ratio = n/n_0

— accumulated number of load cycles when passing through the barred speed range, N_C is assumed to be less than 10^5 for this plant since the passage is with zero pitch.
— permissible low cycle torsional vibratory stress, τ_{vLC}, as calculated above:

$$\tau_{vLC} = 66.2 - 0.15\lambda^2\, 23.77\ \mathrm{N/mm^2}$$
$$= 66.2 - 3.57\,\lambda^2\ \mathrm{N/mm^2}$$

Consequently:
The permissible torsional vibratory stress in transient condition as a function of shaft speed is then:

$$\tau_{vT} \le (22.4 - 0.08\,\lambda^2)\,30^{0.4\log\left(\frac{66.2-3.57\lambda^2}{22.4-0.08\lambda^2}\right)}\ \mathrm{N/mm^2}$$

This is then plotted as a function of engine speed in the calculated torsional vibration diagram:, see Figure 9.

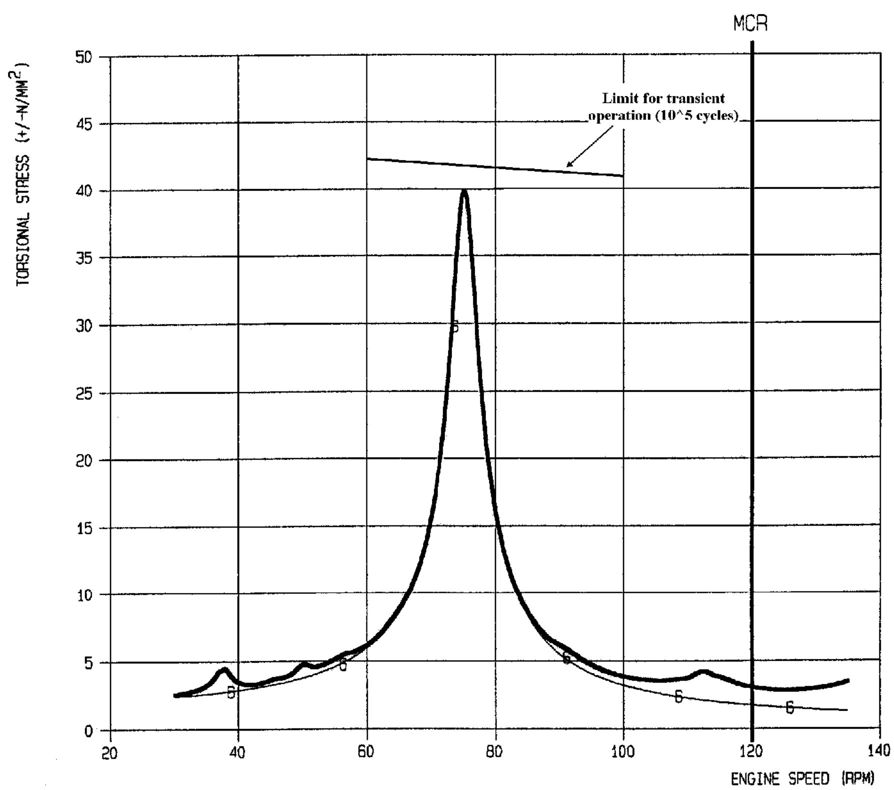

Figure 9 Calculated steady state torsional vibration stress with 0-pitch and stress limit for transient operation

Conclusion:

If we compare the stress limit for transient operation with the calculated steady state stress, we see from Figure 9 that the limit is almost reached at 74 r.p.m. However, when quickly passing the barred speed range with 0-pitch, the stresses will not have sufficient time to build up to the calculated steady state level. Also the expected number of cycles of significant load may be lower than the assumed 10^5 when quickly passing through the barred speed range. This shall be verified by measurements on board during sea trials or be based on experience with similar plants.

The measured shaft stresses converted to the O.D. shaft during the sea trials when passing quickly through the barred speed range with zero pitch are shown on Figure 10. The engine was taken up to 64 r.p.m with zero pitch and kept there some seconds. Then the engine was brought as quickly as possible with zero pitch through the barred speed range to 90 r.p.m, see Figure 10.

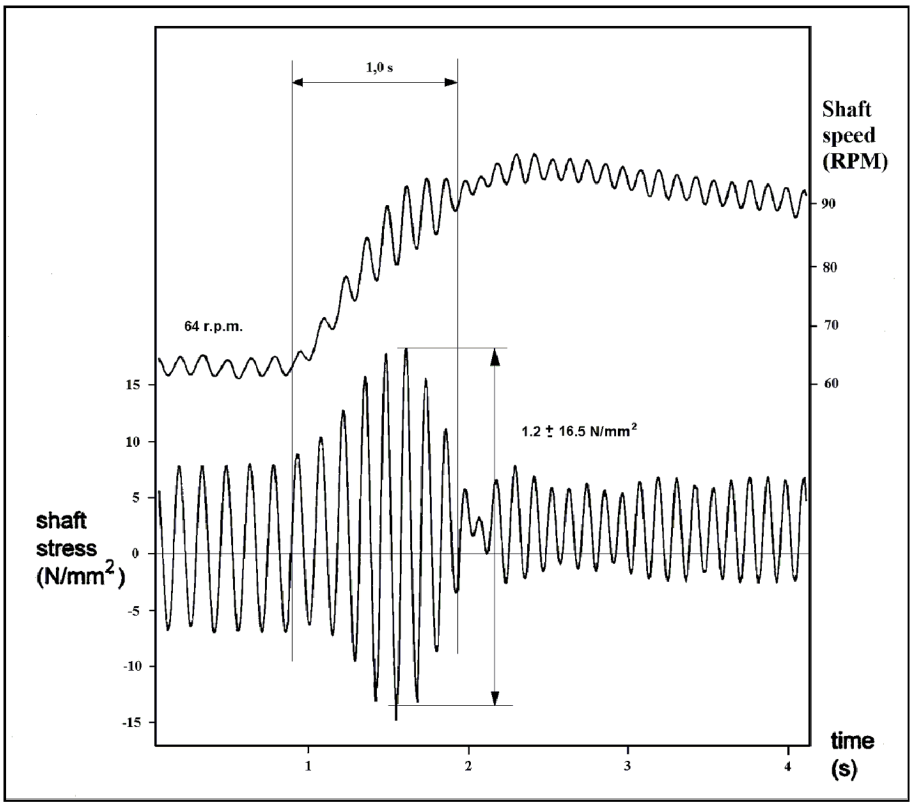

Figure 10 Measured transient torsional stress

Measurements were also carried out when slowing down through the barred speed range, showing similar stress cycles.

From these measurements one can observe the following:

a) The maximum torsional vibratory stress amplitude is 16.5 N/mm^2, which is 41% of the calculated steady state amplitude.

b) The equivalent number of cycles N_c with 100% amplitude for one passage up and down are calculated according to item Sec.5 [2.1] 6) assuming that the number of cycles for starting is the same as for stopping:

$$N_e = 2 \cdot \left(N_{100} + \frac{N_{90}}{1{,}3^{\left(\frac{1}{\log\frac{\tau_{vLC}}{\tau_{vHC}}}\right)}} + \frac{N_{80}}{1{,}7^{\left(\frac{1}{\log\frac{\tau_{vLC}}{\tau_{vHC}}}\right)}} + \frac{N_{70}}{2{,}4^{\left(\frac{1}{\log\frac{\tau_{vLC}}{\tau_{vHC}}}\right)}}\right) = 2 \cdot \left(2 + \frac{2}{1.3^{\left(\frac{1}{\log\frac{64.84}{22.37}}\right)}} + \frac{0}{1.7^{\left(\frac{1}{\log\frac{64.84}{22.37}}\right)}} + \frac{1}{2.4^{\left(\frac{1}{\log\frac{64.84}{22.37}}\right)}}\right) = 2 \cdot (2 + 1.1 + 0 + 0.15) \approx 7$$

The accumulated number of cycles N_c is then calculated as N_e times expected number of passages during the ships life-time, see Sec.5 [2.1]:

Once every week, i.e. 1000 passages, gives N_c = 7000 load cycles, which is far less than the assumed 10^5 load cycles.

Consequently, also the transient vibration criterion is fulfilled.

3 Calculation example 3: Intermediate shaft in a direct coupled, fixed pitch plant with no ice-class:

The shaft arrangement is shown in Figure 11.

Main engine: 5 cylinder MAN B&W 5L70MCE rated to 9000 kW at 105 r.p.m.

A Viscous type torsional vibration damper is mounted and the diameter of the fixed pitch propeller is 7.0 m.

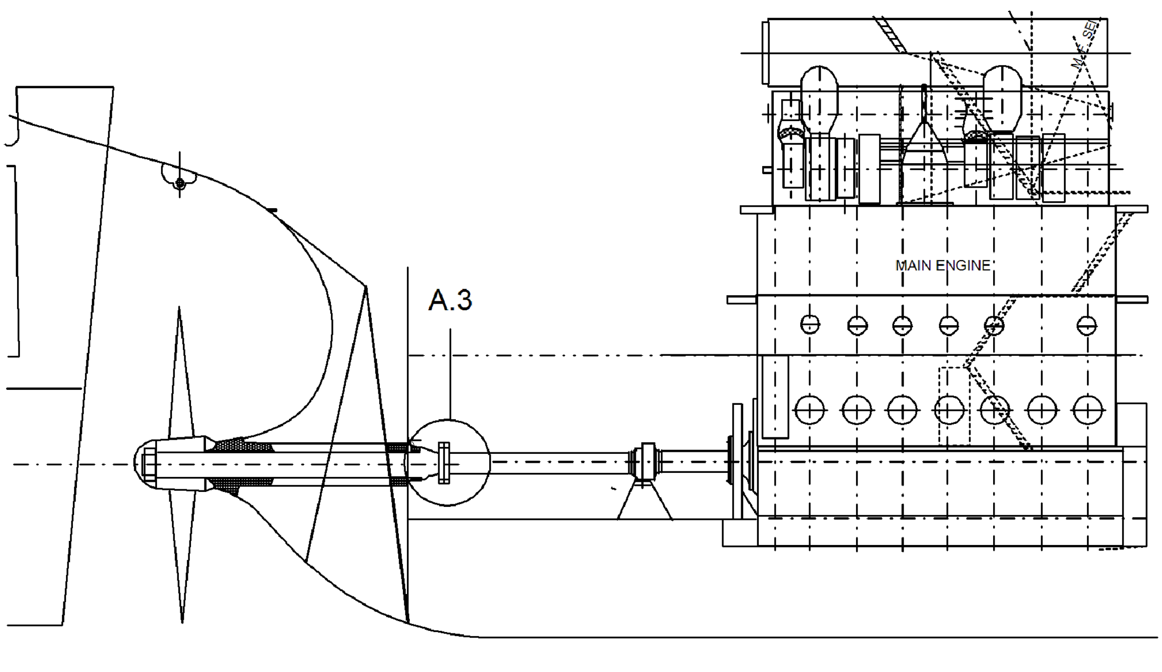

Figure 11 Direct coupled fixed pitch propeller plant

3.1 In way of flange fillet of the intermediate shaft, first design proposal:

First proposal for intermediate shaft design is a 500 mm diameter shaft with a flange fillet of multiradii design made from unalloyed carbon steel JIS G3201 SF 590 A. Other relevant dimensions are shown in Figure 12.

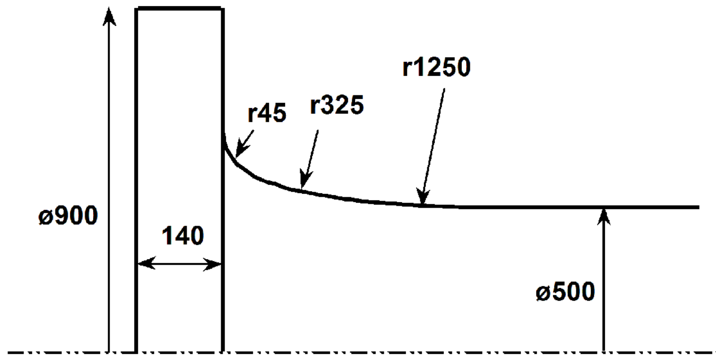

Figure 12 Intermediate shaft flange fillet for ø500 mm shaft

Relevant loads:

— torque at maximum continuous power, T_0 = 818.5 kNm at 105 r.p.m.
— negligible rotating bending moment (to be confirmed by shaft alignment analysis)
— calculated steady state torsional vibrations according to Figure 13.

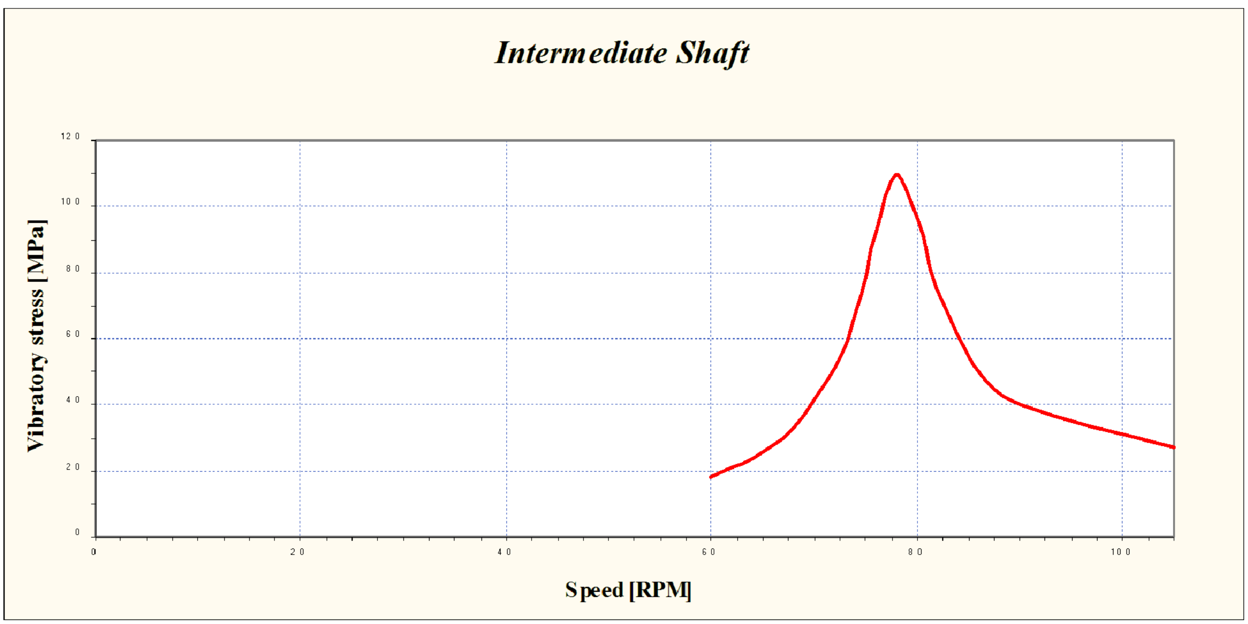

Figure 13 Torsional vibration calculations in normal condition with ø500 mm shaft

Relevant dimensions:

— outer diameter, d = 500 mm
— multiradii transition, see Figure 12 and Sec.6 Table 1
— flange thickness, t = 140 mm
— flange diameter, D = 900 mm
— surface roughness in flange fillet, R_a = 1.6 μm, i.e. R_y = 9.6 μm

Relevant material data:

— steel JIS G3201 SF 590 A with the following minimum mechanical properties for representative test pieces[8]:
 ultimate tensile strength, $\sigma_B \geq 590$ N/mm^2
 yield strength, $\sigma_y \geq 295$ N/mm^2

Calculations:

The Low Cycle Criteria (see Sec.3 [2]):

a) Peak stress:

$$\tau_{max} = (\tau + \tau_v)_{max} \leq \frac{\sigma_y}{2SK_L}$$

— nominal torsional stress at maximum continuous power (see Sec.3 [3]):

$$\tau_0 = \frac{16 \cdot 818.5 \cdot 10^6}{\pi \cdot 500^3} \text{N/mm}^2 = 33.35 \text{ N/mm}^2$$

— maximum value of $(\tau + \tau_v)$ in the entire speed range (see Sec.3 [3]):

the peak torque in misfiring condition will be lower than in normal condition since the engine speed and engine load will be reduced to 86% and 63% of maximum continuous rating (MCR) respectively.

Therefore, in this case there are two potential maximum values of $(\tau + \tau_v)$:

i) running at n_0 = 105 r.p.m in normal condition: Nominal torsional stress: τ_0 = 33.35 N/mm^2 and vibratory torsional stress (see Figure 13): τ_v = 26.9 N/mm^2. Thus, in this case $(\tau + \tau_v)$ = 60.25 N/mm^2

ii) running (accidently[9]) at 5th order resonance speed = 78 r.p.m:
 nominal torsional stress at 78 r.p.m:

$$\tau_{78r.p.m.} = \left(\frac{78}{105}\right)^2 33.35 \text{ N/mm}^2 = 18.4 \text{ N/mm}^2$$

Vibratory torsional stress (steady state) at 78 r.p.m is according to the torsional vibration calculations (see Figure 13): $\tau_{v78 \text{ r.p.m.}}$=109 N/mm^2. Thus, in this case $(\tau + \tau_v)$ = 128.0 N/mm^2.

The maximum torsional stress occurs in case ii):

$$(\tau + \tau_v)_{max} = (\tau + \tau_v)_{78r.p.m.} = 128.0 \text{ N/mm}^2$$

— yield strength:
 σ_y = 295 N/mm^2

---

8 See DNVGL-RU-SHIP Pt.2 Ch.2 Sec.6.

9 Accidently, since running steady at 78 r.p.m is not relevant as the high cycle criterion below concludes with a barred speed range around 78 r.p.m. However, passing through a barred speed range in this l-range will result in transient torsional vibrations close to the steady state level.

— safety factor (see DNVGL-RU-SHIP Pt.4 Ch.4 Sec.1 [2.2.3]): S = 1.25

— geometrical stress concentration factor, torsion according to Sec.6 Table 1 in Sec.6 [2]:

α_t = 1.05

— component influence factor for low cycle fatigue (see Sec.3 [5]):

$$K_L = 1 + (1.05 - 1)\frac{295}{900} + 10^{-4}(590 - 200)\log 9.6 = 1.05$$

Consequently:

$$128.0\ \mathrm{N/mm^2} > \frac{295}{2 \cdot 1.25 \cdot 1.05}\ \mathrm{N/mm^2} = 112.4\ \mathrm{N/mm^2}$$

or actual safety factor, S = 1.1

Conclusion:

The above calculation is somewhat on the conservative side since the allowable stresses are compared with the peak stresses taking the calculated steady state vibratory stresses at 78 r.p.m. into account. Since a certain speed range around 78 r.p.m. will be barred for continuous running due to the high cycle criterion below, the actual vibratory stresses will be slightly lower than the calculated ones. This shall be confirmed by measurements. See also conclusion to the transient criterion below.

b) Torque reversal:

$$\alpha_t \Delta\tau \le \frac{2\sigma}{S\sqrt{3}}$$

— repetitive nominal torsional stress range due to reversing (see Sec.3 [4]):

$$\Delta\tau \approx 2(\tau + \tau_v) = 2 \cdot 128\ \mathrm{N/mm^2} = 256.0\ \mathrm{N/mm^2}$$

— safety factor (see DNVGL-RU-SHIP Pt.4 Ch.4 Sec.1 [2.2.3]):

S = 1.25

Consequently:

$$1.05 \cdot 256.0\ \mathrm{N/mm^2} \le \frac{2 \cdot 295}{1.25 \cdot \sqrt{3}}\ \mathrm{N/mm^2}$$

$$\Updownarrow$$

$$268.8\ N/mm^2 \leq 272.5 N/mm^2$$

or actual safety factor 1.27

Conclusion:

Criterion fulfilled.

The high cycle criterion (see Sec.4 [2]):

$$\left(\frac{\tau_v}{\tau_f}\right)^2 + \left(\frac{\sigma_b}{\sigma_f}\right)^2 \leq \frac{1}{S^2}$$

— notch sensitivity coefficient for high cycle torsional fatigue (see Sec.4 [4.1]): m_t=1.0 due to multiradii transition

— component influence factor for high cycle torsional fatigue (see Sec.4 [4]):

$$K_{H\tau} = \frac{1.05}{1.0} + 0,01\sqrt{100} + 3 \cdot 10^{-4}(590 - 200)\log 9.6 = 1.26$$

— high cycle torsional fatigue strength (see Sec.4 [3]):

$$\tau_f = \frac{0.24 \cdot 295 + 42 - 0.15\lambda^2 33.35}{1.26}\ N/mm^2 =$$

$$89.5 - 3.97 \cdot \lambda^2\ N/mm^2$$

λ is the speed ratio = n/n_0

— $\left(\frac{\sigma_b}{\sigma_f}\right)^2 \approx 0$ since rotating bending moment is negligible at this section of the shaft

— safety factor (see DNVGL-RU-SHIP Pt.4 Ch.4 Sec.1 [2.2.3]):
S = 1.6

Consequently:

The permissible torsional vibratory stress as a function of shaft speed is then:

$$\tau_{vHC} \leq \frac{89.5 - 3.97\lambda^2}{1.6} N/mm^2 = 55.9 - 2.48\lambda^2\ N/mm^2$$

This is then plotted as a function of engine speed in the calculated torsional vibration diagram, see Figure 14:

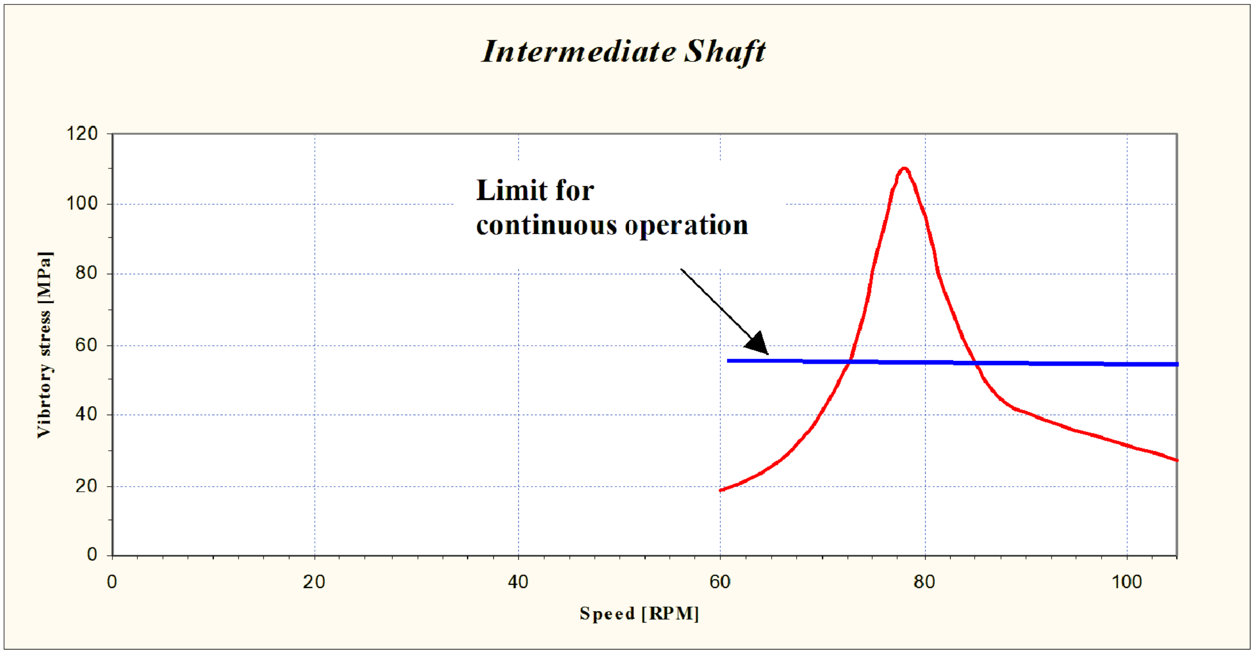

Figure 14 Calculated steady state torsional vibrations stress and stress limit for continuous operation with ø500 mm shaft.

Conclusion:

The calculated stresses are higher than the allowable stresses for continuous operation around the 5^{th} order resonance at 78 r.p.m. In this case it means that a relatively wide barred speed range shall be introduced from 72 to 84 r.p.m. According to the rules, the barred speed range can not be introduced in the operational range above 0.8 n_0 = 84 r.p.m.

The Transient Vibration Criterion (see Sec.5):

— permissible high cycle torsional vibration stress, τ_{vHC}, as calculated above but with a safety factor of 1.5:

$$\tau_{vT} \leq \tau_{vHC}\left(\frac{3 \cdot 10^6}{N_C}\right)^{0.4\log\left(\frac{\tau_{vLC}}{\tau_{vHC}}\right)} = \tau_{vLC}\left(\frac{N_C}{10^4}\right)^{0.4\log\left(\frac{\tau_{vHC}}{\tau_{vLC}}\right)}$$

$$\tau_{vHC} = \frac{89.5 - 3.97\lambda^2}{1.5} N/mm^2 = 59.7 - 2.65\lambda^2 \ N/mm^2$$

λ is the speed ratio = n/n_0

— accumulated number of load cycles when passing through the barred speed range, N_C is assumed to be at least 10^5 for this plant since the passage is with fixed pitch and the barred speed range is in the upper region of the λ-range.

— permissible low cycle torsional vibratory stress, τ_{vLC}, as calculated above:

$$\tau_{vLC} = 112.4 - 33.35\lambda^2 \text{ N/mm}^2$$

Consequently:

The permissible torsional vibratory stress in transient condition as a function of shaft speed is then:

$$\tau_{vT} \leq \left(59.7 - 2.65\lambda^2\right) 30^{0.4\log\left(\frac{112.4 - 33.35\lambda^2}{59.7 - 2.65\lambda^2}\right)} N/mm^2$$

This is then plotted as a function of engine speed in the calculated torsional vibration diagram, see Figure 15:

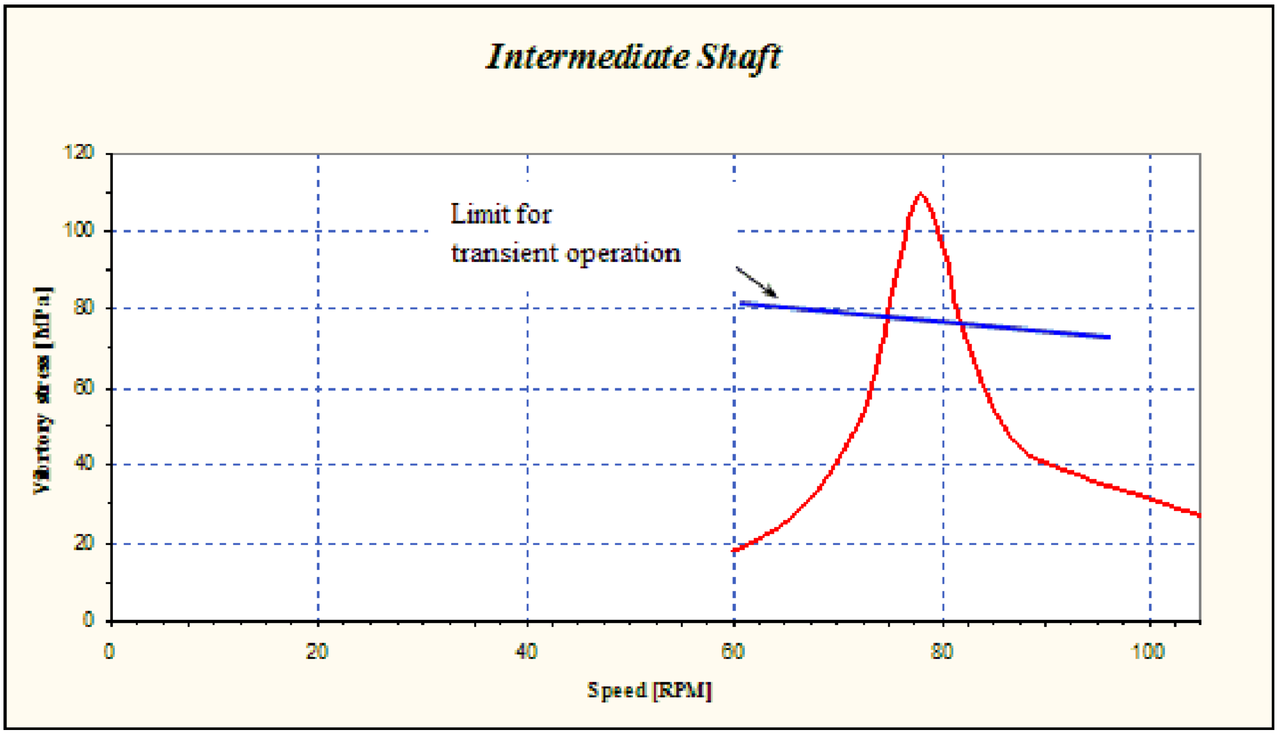

Figure 15 Calculated steady state torsional vibrations stress and stress limit for transient operation with ø500 mm shaft.

Conclusion:

If we compare the limit for the transient operation with the calculated steady state stresses around 78 r.p.m, we see from Figure 15 that the limit is exceeded by 44%. Since the barred speed range is in the upper speed range and this is a fixed pitch propeller plant, it is not possible to "quickly" pass this barred speed range. The stresses will have sufficient time to build up to the steady state level and the accumulated number of cycles will be relatively high. In this case it is also unlikely that the peak stress criterion above will be fulfilled. Therefore the intermediate shaft design should be changed or alternatively a very much larger damper to be fitted. Of cost reason the last alternative is not further pursued.

It is of course possible to only change the material to a material with better mechanical properties, but in order to move the barred speed range down so that the accumulated load cycles will be fewer, the shaft diameter should also be reduced. This has also another benefit with regards to shaft alignment since the shaft line will be more flexible.

3.2 In way of flange fillet of the intermediate shaft, second design proposal:

Second proposal for intermediate shaft design for the same plant is a 380 mm diameter shaft with the same multiradii flange transition as the first proposal, but made from quenched and tempered alloyed steel EN10083-1 - 34CrNiMo6 +QT. Other relevant dimensions are shown in Figure 16.

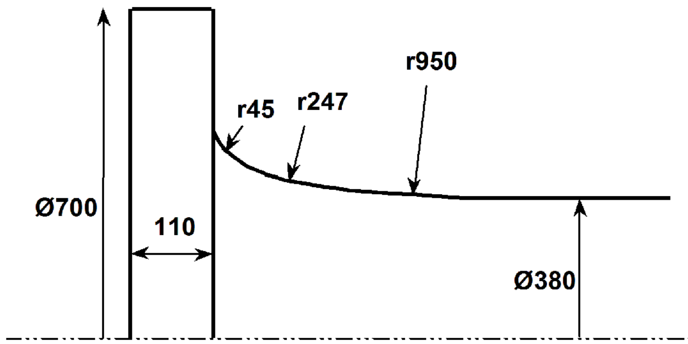

Figure 16 Intermediate shaft flange fillet for ø380 mm shaft

Relevant loads:

— since the shaft stiffness has been reduced, the calculated steady state torsional vibrations have been changed according to Figure 17.

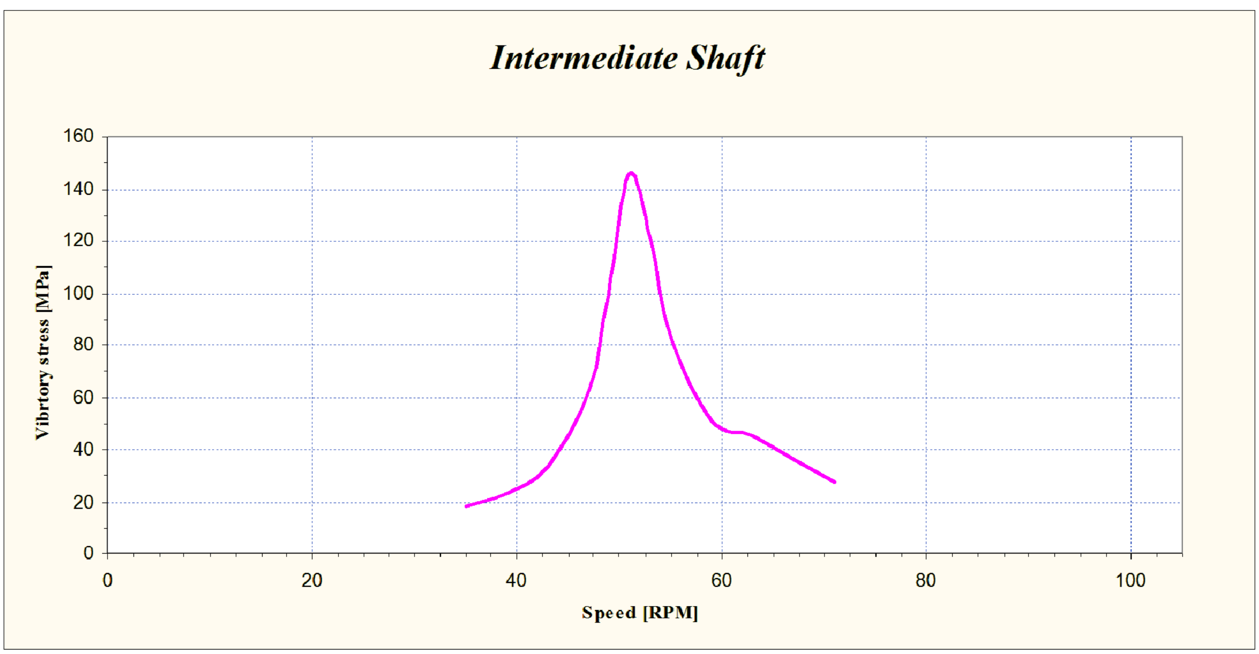

Figure 17 Torsional vibration calculations in normal condition with ø380 mm shaft

Relevant dimensions:

— outer diameter, d = 380 mm
— multiradii transition, see Figure 16 and Sec.6 Table 1
— flange thickness, t = 110 mm
— flange diameter, D = 700 mm
— surface roughness in flange fillet, R_a = 1.6 µm, i.e. R_y = 9.6 µm

Relevant material data:

— ouenched and tempered alloyed steel EN10083-1 34CrNiMo6 +QT with the following minimum mechanical properties for representative test pieces[10]:
ultimate tensile strength, $\sigma_B \geq 900$ N/mm^2
yield strength, $\sigma_y \geq 700$ N/mm^2

Calculations:

The Low Cycle Criteria (see Sec.3 [2]):

a) Peak stress:

$$\tau_{max} = (\tau + \tau_v)_{max} \leq \frac{\sigma_y}{2SK_L}$$

— nominal torsional stress at maximum continuous power (see Sec.3 [3]):

$$\tau_0 = \frac{16 \cdot 818.5 \cdot 10^6}{\pi 380^3} \text{ N/mm}^2 = 75.97 \text{ N/mm}^2$$

— maximum value of ($\tau + \tau_v$) in the entire speed range (see Sec.3 [3]) will be when running (accidently[11]) at 5th order resonance speed = 51 r.p.m.:
nominal torsional stress at 51 r.p.m:

$$\tau_{51 r.p.m.} = \left(\frac{51}{105}\right)^2 75.97 \text{ N/mm}^2 = 17.9 \text{ N/mm}^2$$

vibratory torsional stress (steady state) at 51 r.p.m is according to the torsional vibration calculations (see Figure 17):

$\tau_{v51r.p.m.}$= 145.7 N/mm^2

thus, in this case $(\tau + \tau_v)_{max}$ = 163.6 N/mm^2.

— yield strength:
σ_y=700 N/mm^2, however limited to 0.7σ_B= 630 N/mm^2 in the fatigue strength calculation.

— safety factor (see DNVGL-RU-SHIP Pt.4 Ch.4 Sec.1 [2.2.3]):
S=1.25

---

10 See DNVGL-RU-SHIP Pt.2 Ch.2 Sec.66

11 Accidently, since running steady at 51 r.p.m. is not relevant as the high cycle criterion below concludes with a barred speed range around 51 r.p.m. Using the steady state vibration level is a conservative assumption in this case since passing through the barred speed range with $\ell \leq 0.5$ will happen quickly and the transient vibration level will normally be approximately 80% of the steady state level.

— geometrical stress concentration factor, torsion according to Sec.6 Table 1 in Sec.6 [2]:
$\alpha_t = 1.05$

— component influence factor for low cycle fatigue (see Sec.3 [5]):

$$K_L = 1 + (1.05 - 1)\left(\frac{700}{900} + 10^{-4}(900 - 200)\log 9.6\right) = 1.11$$

Consequently:

$$163.6\ \mathrm{N/mm^2} \le \frac{630}{2 \cdot 1.25 \cdot 1.11}\mathrm{N/mm^2} = 227\ \mathrm{N/mm^2}$$

or actual safety factor, S = 1.7

Conclusion:

Criterion fulfilled.

b) Torque reversal:

$$\alpha_t \Delta\tau \le \frac{2\sigma_y}{S\sqrt{3}}$$

— repetitive nominal torsional stress range due to reversing (see Sec.3 [4]):

$$\Delta\tau \approx 2(\tau + \tau_v) = 2 \cdot 163.6\ \mathrm{N/mm^2} = 327.2\ \mathrm{N/mm^2}$$

— safety factor (see DNVGL-RU-SHIP Pt.4 Ch.4 Sec.1 [2.2.3]):
S = 1.25

Consequently:

$$1.05 \cdot 327.2\ \mathrm{N/mm^2} \le \frac{2 \cdot 630}{1.25\sqrt{3}}\ \mathrm{N/mm^2}$$

$$\Updownarrow$$

$$343.6\ \mathrm{N/mm^2} \le 582\ \mathrm{N/mm^2}$$

or actual safety factor 2.12

Conclusion:

Criterion fulfilled.

The high cycle criterion (see Sec.4 [2]):

$$\left(\frac{\tau_v}{\tau_f}\right)^2 + \left(\frac{\sigma_b}{\sigma_f}\right)^2 \leq \frac{1}{S^2}$$

— notch sensitivity coefficient for high cycle torsional fatigue (see Sec.4 [4.1]):
  m_t = 1.0 d due to multiradii transition
— component influence factor for high cycle torsional fatigue (see Sec.4 [4]):

$$K_{H\tau} = \frac{1.05}{1.0} + 0.01\sqrt{100} + 3 \cdot 10^{-4}900 - 200\log 9.6 = 1.36$$

— high cycle torsional fatigue strength (see Sec.4 [3]):

$$\tau_f - \frac{0.24 \cdot 630 + 42 - 0.15\lambda^2 75.97}{1.36}\ \mathrm{N/mm^2}$$

$$= 142.1 - 8.38\lambda^2\ \mathrm{N/mm^2}$$

λ is the speed ratio = n/n_0

— $\left(\frac{\sigma_b}{\sigma_f}\right)^2 \approx 0,$ since rotating bending moment is negligible at this section of the shaft

— safety factor (see DNVGL-RU-SHIP Pt.4 Ch.4 Sec.1 [2.2.3]):
  S = 1.6

Consequently:

The permissible torsional vibratory stresses as a function of shaft speed is then:

$$\tau_{vHC} \leq \frac{142.1 - 8.38\lambda^2}{1.6} = 88.8 - 5.2\lambda^2\ \mathrm{N/mm^2}$$

This is then plotted as a function of engine speed in the calculated torsional vibration diagram, see Figure 18:

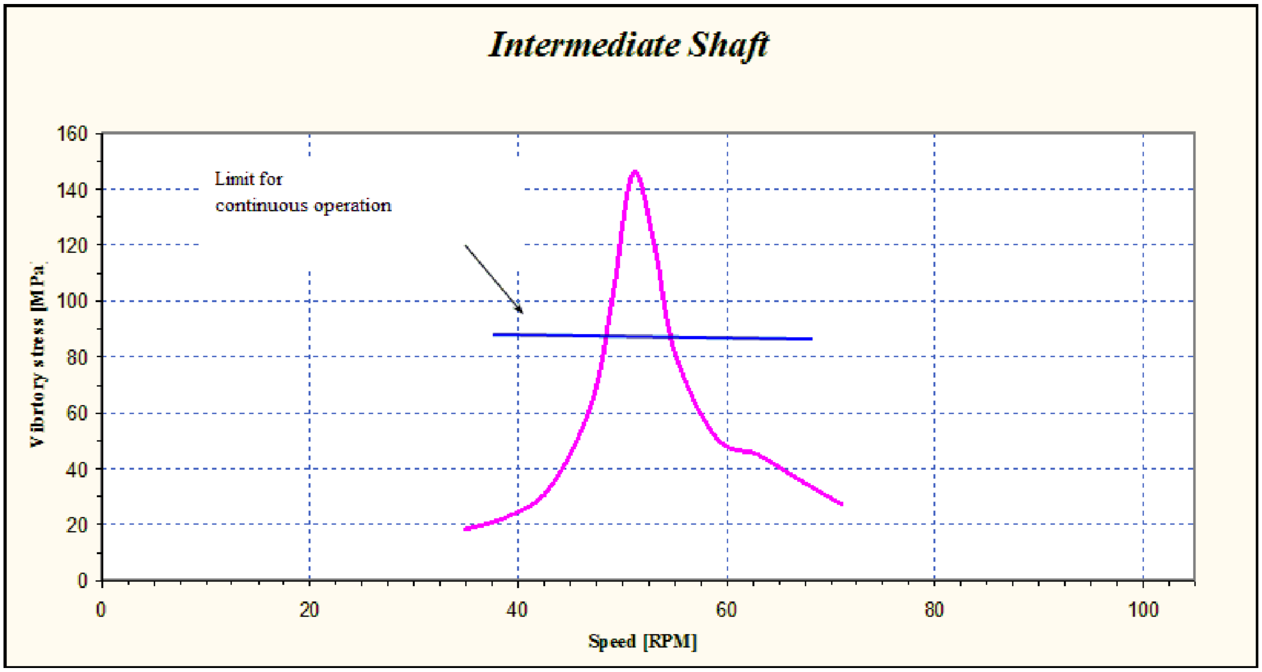

Figure 18 Calculated steady state torsional vibrations stress and stress limit for continuous operation with ø380 mm shaft.

Conclusion:

The calculated stresses are higher than the allowable stresses for continuous operation around the 5th order resonance at 51 r.p.m. A barred speed range shall be introduced from 48 to 56 r.p.m. However, the barred speed range should be confirmed by torsional vibration measurements on board during the sea trials.

The Transient Vibration Criterion (Sec.5):

$$\tau_{vT} \leq \tau_{vHC}\left(\frac{3 \cdot 10^6}{N_C}\right)^{0.4\log\left(\frac{\tau_{vLC}}{\tau_{vHC}}\right)}$$

$$= \tau_{vLC}\left(\frac{N_C}{10^4}\right)^{0.4\log\left(\frac{\tau_{vHC}}{\tau_{vLC}}\right)}$$

where:

— permissible high cycle torsional vibration stress, τ_{vHC}, as calculated above but with a safety factor of 1.5:

$$\tau_{vHC} = \frac{142.1 - 8.38\lambda^2}{1.5}\ N/mm^2 = 94.7 - 5.59\lambda^2\ N/mm^2$$

λ is the speed ratio = n/n_0

— accumulated number of load cycles when passing through the barred speed range, N_C is assumed to be reduced to $5 \cdot 10^4$ in this case since the barred speed range has been moved down in the speed range.

— permissible low cycle torsional vibratory stress, τ_{vLC}, as calculated above:

$$\tau_{vLC} = 227 - 75.97\lambda^2 \ \mathrm{N/mm^2}$$

Consequently:

The permissible torsional vibratory stresses in transient condition as a function of shaft speed is then:

$$\tau_{vT} \leq \left(94.7 - 5.59 \cdot \lambda^2\right) \cdot 30^{0.4 \cdot \log\left(\frac{227 - 75.97 \cdot \lambda^2}{94.7 - 5.59 \cdot \lambda^2}\right)} \ \mathrm{N/mm^2}$$

This is then plotted as a function of engine speed in the calculated torsional vibration diagram, see Figure 19:

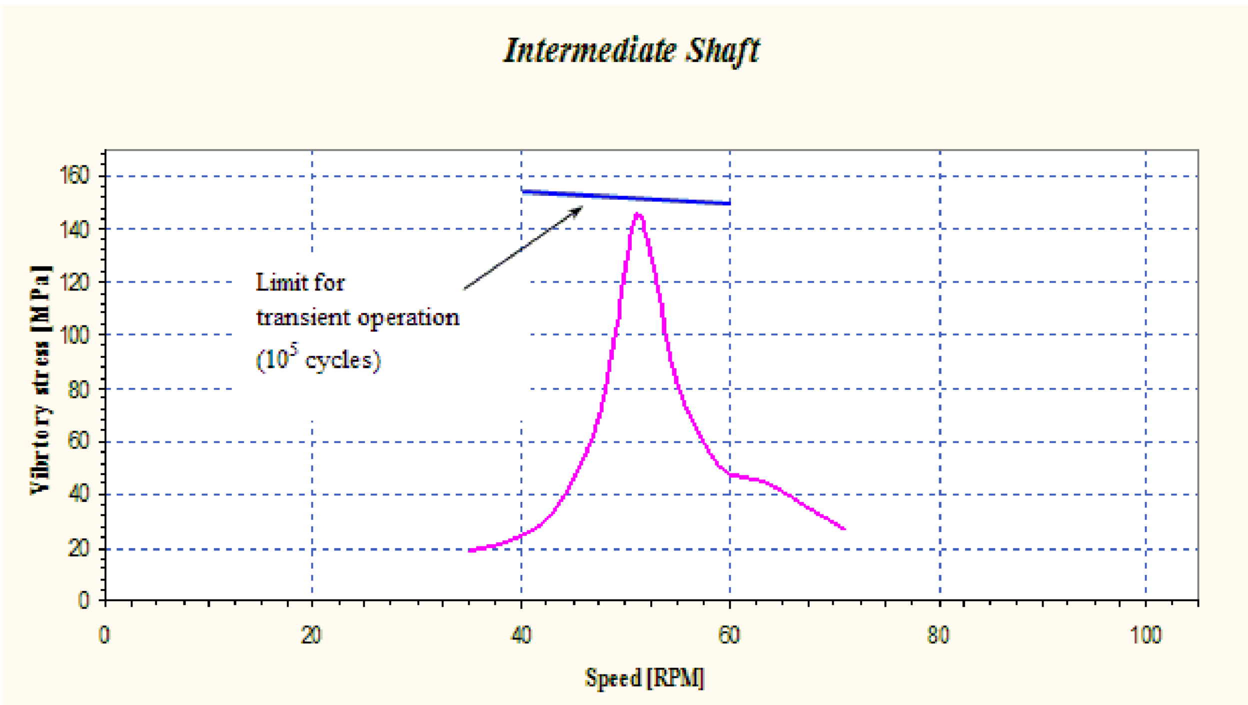

Figure 19 Calculated steady state torsional vibrations stress and stress limit for transient operation with ø380 mm shaft.

Conclusion:

If we compare the stress limit for transient operation with the calculated steady state stress, we see from Fig. A-19 that the limit is just reached at 51 r.p.m. However, when quickly passing the barred speed range, the stresses will certainly not be as high as the calculated steady state stresses. This shall be verified by measurements on board during sea trials or be based on experience with similar plants.

The measured shaft stresses during the sea trials for this plant are presented in Figure 20 and Figure 21.

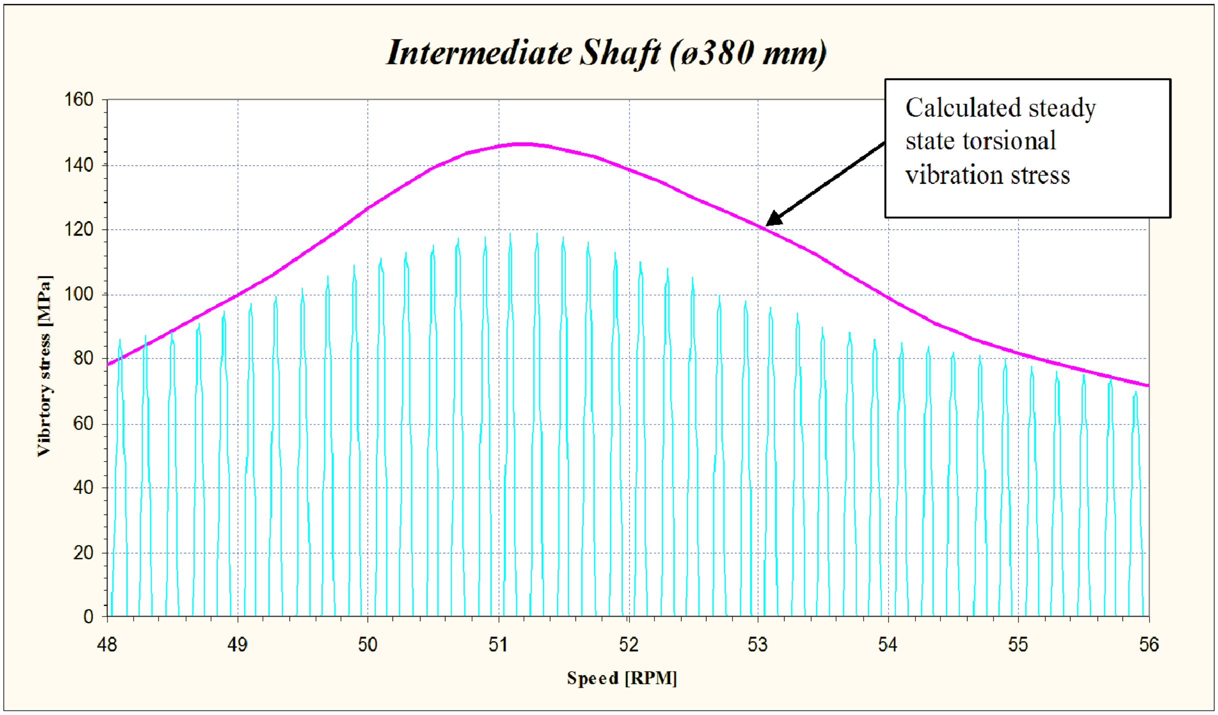

Figure 20 Measured stresses with respect to shaft speed.

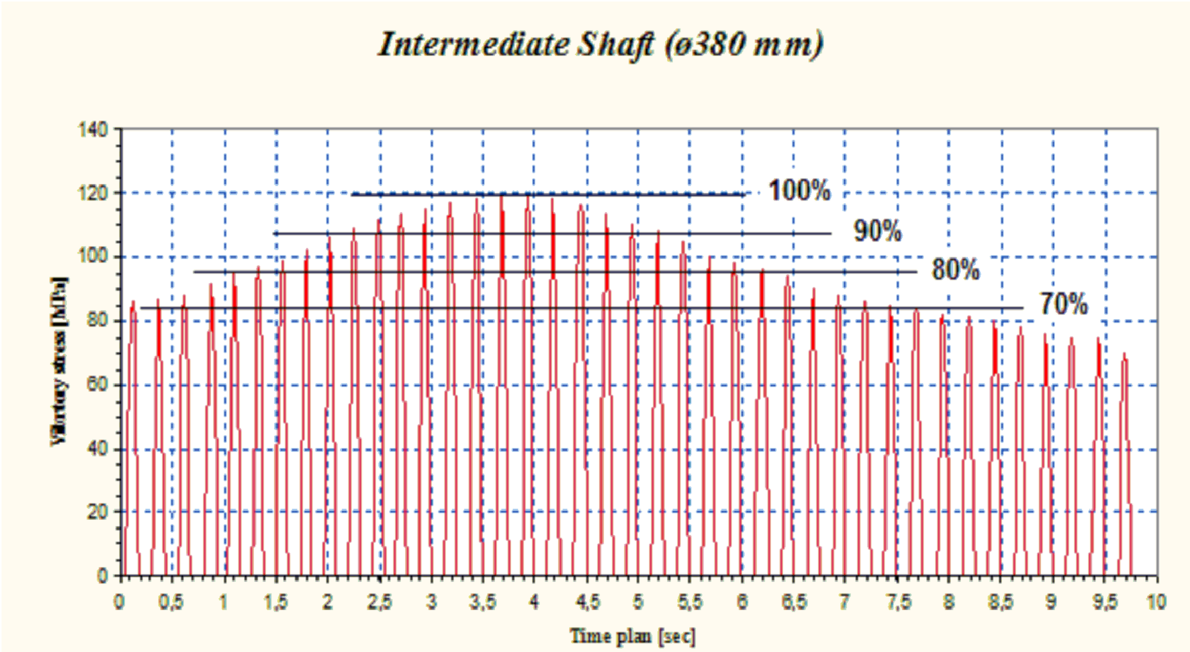

Figure 21 Measured stresses with respect to time

From these measurements one can observe the following:

a) The maximum torsional vibratory stress amplitude is 120 N/-mm^2, which is 82% of the calculated steady state amplitude.

b) The equivalent number of cycles, N_e with 100% amplitude for one passage up and down are calculated according to Sec.5 [2.1].6) assuming that the number of cycles for starting is the same as for stopping.

$$\tau_{vLC} = 227 - 75.97 \cdot \left(\frac{51}{105}\right)^2 \ \text{N/mm}^2 = 209.1 \ \text{N/mm}^2$$

$$\tau_{vHC} = 94.7 - 5.59 \cdot \left(\frac{51}{105}\right)^2 \ \text{N/mm}^2 = 93.4 \ \text{N/mm}^2$$

$$N_e = 2N_{100} + \frac{N_{90}}{1,3^{\left(\frac{1}{\log\frac{\tau_{vLC}}{\tau_{vHC}}}\right)}} + \frac{N_{80}}{1,7^{\left(\frac{1}{\log\frac{\tau_{vLC}}{\tau_{vHC}}}\right)}} = 2 \cdot \left(13 + \frac{8}{1,3^{\left[\frac{1}{\log\frac{209.1}{93.4}}\right]}} + \frac{11}{1,7^{\left[\frac{1}{\log\frac{209.1}{93.4}}\right]}}\right) = 2 \cdot (13 + 3.8 + 2.4) \approx 38.$$

The accumulated number of cycles N_c is then calculated as N_e times expected number of passages during the ships life-time, see Sec.5 [2.1]:

Once every week, i.e. 1000 passages, gives N_c = 38 000 load cycles, which is slightly less than the assumed $5 \cdot 10^4$ load cycles.

Consequently, also the transient vibration criterion is fulfilled.

3.3 In way of flange fillet of the intermediate shaft, using simplified method:

Since this shaft has a flange transition with a multiradii design, the simplified diameter formulae in the DNVGL-RU-SHIP Pt.4 Ch.4 Sec.1 [2.2.8] may be used:

The minimum shaft diameter is:

$$d \geq 100 k \sqrt[3]{\left(\frac{P}{n_0} \frac{560}{\sigma_B + 160}\right)}$$

$$= 100 \cdot 1.0 \cdot \sqrt[3]{\left(\frac{9000}{105} \frac{560}{590 + 160}\right)} \text{ mm} = 400 \text{ mm}$$

However, the shaft diameter shall also fulfill the criteria for torsional vibration:

a) For continuous operation (high cycle fatigue):

for $\lambda \geq 0.9$:

$$\tau_1 = \frac{\sigma_B + 160}{18} C_k C_d 1.38$$

$$= \frac{590 + 160}{18} 1.0 \cdot 0.35 + 0.93 \cdot 400^{(-0.2)} 1.38 \text{ N/mm}^2$$
$$= 36.3 \text{ N/mm}^2$$

for $\lambda < 0.9$:

$$\tau_1 = \frac{\sigma_B + 160}{18} C_k C_d (3 - 2\lambda^2)$$

$$= \frac{590 + 160}{18} 1.0 (0.35 + 0.93 \cdot 400^{-0.2})(3 - 2\lambda^2) \text{N/mm}^2$$

$$= 78.8 - 52.5\lambda^2 \ \mathrm{N/mm^2}$$

b) For transient operation (passing barred speed range):

$$\tau_2 = 1.7\frac{\tau_1}{\sqrt{c_k}} = 1.7\frac{(78.8 - 52.5\lambda^2)}{1.0} \ \mathrm{N/mm^2} \quad = 134.0 - 88.7\lambda^2 \ \mathrm{N/mm^2}$$

These curves are plotted together with the torsional vibration calculations, see Figure 22.

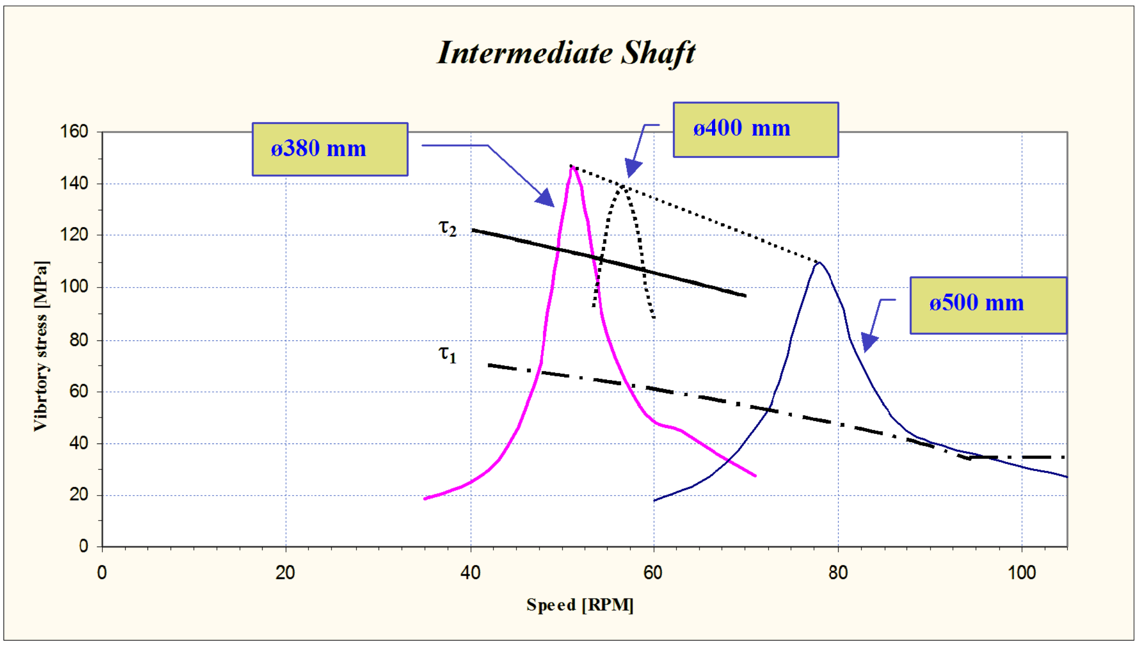

Figure 22 Torsional vibration calculations in normal condition with ø400 mm shaft.

For a 400 mm diameter shaft the 5th order resonance will be around 56 r.p.m and the vibration level is found by interpolation between the levels with 380 mm and 500 mm diameter shafts.

Conclusion:

Figure 22 shows that for a 400 mm diameter shaft the calculated vibration stress exceeds the permissible stress in transient condition. For the simplified criteria, the permissible transient stresses shall be compared with steady state vibrations and not the actual transient vibrations as for the detailed criteria above. The shaft diameter can not be reduced because the criterion for minimum diameter shall be met, and the diameter can not be increased either since the permissible stresses will never exceed the calculated steady state vibrations. The only possibilities left are to introduce a high strength material or to install a larger damper. The transient criterion will be fulfilled if the tensile strength is increased to:

$$\sigma_B \geq \frac{140}{105}(590 + 160) - 160 \ \mathrm{N/mm^2} = 840 \ \mathrm{N/mm^2}$$

This means that the material shall be changed from carbon steel to quenched and tempered alloyed steel.

CHANGES – HISTORIC

December 2015 edition

This is a new document.

About DNV GL

DNV GL is a global quality assurance and risk management company. Driven by our purpose of safeguarding life, property and the environment, we enable our customers to advance the safety and sustainability of their business. We provide classification, technical assurance, software and independent expert advisory services to the maritime, oil & gas, power and renewables industries. We also provide certification, supply chain and data management services to customers across a wide range of industries. Operating in more than 100 countries, our experts are dedicated to helping customers make the world safer, smarter and greener.

SAFER, SMARTER, GREENER